Too Afraid to Drive: Systematic Discovery of Semantic DoS Vulnerability in Autonomous Driving Planning under Physical-World Attacks

Ziwen Wan Junjie Shen Jalen Chuang Xin Xia† Joshua Garcia Jiaqi Ma† Qi Alfred Chen
University of California, Irvine †University of California, Los Angeles
{ziwenw8, junjies1, jzchuang, joshua.garcia, alfchen}@uci.edu
†{x35xia, jiaqima}@ucla.edu

***Abstract*—In high-level Autonomous Driving (AD) systems, behavioral planning is in charge of making high-level driving decisions such as cruising and stopping, and thus highly security-critical. In this work, we perform the first systematic study of semantic security vulnerabilities specific to overly-conservative AD behavioral planning behaviors, i.e., those that can cause failed or significantly-degraded mission performance, which can be critical for AD services such as robo-taxi/delivery. We call them semantic Denial-of-Service (DoS) vulnerabilities, which we envision to be most generally exposed in practical AD systems due to the tendency for conservativeness to avoid safety incidents. To achieve high practicality and realism, we assume that the attacker can only introduce seemingly-benign external physical objects to the driving environment, e.g., off-road dumped cardboard boxes.**

To systematically discover such vulnerabilities, we design PlanFuzz, a novel dynamic testing approach that addresses various problem-specific design challenges. Specifically, we propose and identify planning invariants as novel testing oracles, and design new input generation to systematically enforce problem-specific constraints for attacker-introduced physical objects. We also design a novel behavioral planning vulnerability distance metric to effectively guide the discovery. We evaluate PlanFuzz on 3 planning implementations from practical open-source AD systems, and find that it can effectively discover 9 previously-unknown semantic DoS vulnerabilities without false positives. We find all our new designs necessary, as without each design, statistically significant performance drops are generally observed. We further perform exploitation case studies using simulation and real-vehicle traces. We discuss root causes and potential fixes.

I. Introduction

Today, various companies are developing high-level (e.g., Level-4 [1]) Autonomous Driving (AD) vehicles. Some of them, e.g., Google Waymo [2], TuSimple [3], and Pony.ai [4], are already providing services on public roads. To enable such highly-automated driving, after the environmental sensing steps such as perception and localization, the AD systems need to use the sensed information to make high-level driving decisions such as cruising, stopping, lane changing, etc., that not only are safe and efficient, but also conform to driving norms such as traffic rules. Such a decision-making process is commonly referred to as *behavioral planning*, which is highly security critical as any mistakes made in it can directly lead to undesired driving behaviors such as driving too aggressively to cause collisions, or too conservatively to cause unnecessary emergency stops and road blocking. Various prior works studied security vulnerabilities in AD systems with such semantic consequences [5–9], but they mostly focus on environmental sensing errors (e.g., camera/LiDAR object detection [6–9]) instead of planning. There are recent works able to discover semantic planning errors [10], but they (1) are designed for whole-system testing instead of being planning-specific; (2) only consider overly-aggressive behaviors, leaving the overly-conservative side unexplored; and (3) focus on safety instead of security (i.e., lack explicit threat model considerations).

To fill this research gap, in this paper we perform the first AD planning-specific semantic vulnerability discovery. We specifically choose to focus on the more under-explored *overly-conservative* behavioral planning behaviors, especially those that can cause the victim AD vehicle to have a failed or significantly-degraded mission performance (e.g., permanent stop and never reach the destination). We refer to these as *semantic Denial-of-Service (DoS) vulnerabilities* for behavioral planning. We envision that such vulnerabilities can be most generally exposed in practice, based on the hypothesis that behavioral planning in real-world AD systems, especially in production settings, will generally try to be as conservative as possible to avoid any possible safety incidents, which can cause great business reputation and financial damages as in recent fatal accidents for Uber and Tesla [11–14]. In fact, such overly-conservative behaviors have already been observed for many production AD vehicles (e.g., Waymo, Uber, Volvo [15–20]), causing troubles to AD service and traffic flow (§II-B).

Considering the realism and generality of such problems in practice, we set our goal to develop an automated system to systematically discover such vulnerabilities to most generally help address these problems at the AD system development stage. To achieve high practicality and realism, we assume that the attacker can only introduce seemingly-benign external physical objects to the driving environment, e.g., dumped cardboard boxes or parked bikes on the road side, attacker-driven vehicles, etc. Dynamic testing is a promising

Network and Distributed Systems Security (NDSS) Symposium 2022
24-28 April 2022, San Diego, CA, USA
ISBN 1-891562-74-6
https://dx.doi.org/10.14722/ndss.2022.24177
www.ndss-symposium.org

approach to achieve domain-specific vulnerability discovery in general [21–28]. However, none of the existing designs can be directly applied to our problem due to several unique design challenges specific to our problem definition: (C1) Lack of testing oracles to tell whether a change of a planning decision is *overly* conservative or not. For example, directly putting obstacles ahead of the victim to cause DoS is not a vulnerability for behavioral planning; (C2) Need to systematically generate attacker-introduced physical objects following problem-specific physical constraints, e.g., avoiding road regions directly ahead of the victim as explained above; and (C3) Need to obtain fine-grained code-level feedback from the planning decision-making process to guide our vulnerability discovery, which is highly desired for us as the direct behavioral planning output is usually quite discrete (§III-B).

To achieve our goal, we design PlanFuzz, a novel dynamic testing approach that systematically addresses the aforementioned design challenges in an evolutionary testing framework. To address C1, we propose and identify *Planning Invariant (PI)* as the problem-specific testing oracle, which defines a set of constraints for the attacker-introduced physical objects based on common driving norms such that if satisfied, the behavior planning should not give up the desired planning decision. To address C2, we design *PI-aware physical-object generation*, which can systematically enforce the generated testing inputs to conform to both driving norms (e.g., traffic rules) and the PI constraints above, while maintaining diversity and inheritance properties desired for evolutionary testing. To address C3, we design *behavioral planning vulnerability distance* to measure how close the current planning decision is to violate PI and thus trigger a vulnerability in the run time.

We implement a prototype of PlanFuzz and evaluate it on 3 different behavioral planning implementations from two open-source AD systems, Apollo [29] and Autoware [30], which are both practical AD systems with full-stack implementations [31, 32]. We use LGSVL, an industry-grade AD simulator, to generate diverse driving scenarios, which allows us to obtain 11,912 different initial testing seeds in total for 8 different driving scenarios. Using PlanFuzz with these seeds, all 3 behavioral planning implementations are found vulnerable, with 9 previously-unknown semantic DoS vulnerabilities discovered in total. Among them, 8 can prevent the victim from reaching the destination (7 can cause permanent stop), and the remaining 1 can cause emergency stop. We also perform baseline comparisons by replacing different key components in our design, which shows statistically significant performance drops for almost all of the 9 vulnerabilities, leading to over 3.5× average slow-down or even failure in their discoveries. We also manually verified the discovered vulnerabilities and no false positives are generated.

To concretely understand the end-to-end impacts of the discovered vulnerabilities, we further perform 3 vulnerability exploitation case studies by constructing and evaluating real-world attack scenarios using simulation and real-vehicle sensor traces. The results show that the discovered vulnerabilities can cause the AD vehicle running Apollo or Autoware to (1) permanently stop in an empty road or in front of an empty intersection due to completely off-road cardboard boxes or parked bikes; or (2) give up necessary lane changing purely due to a following vehicle without any intention to change lanes. Demos are at our website **https://sites.google.com/view/cav-sec/planfuzz** [33]. We also discuss root causes and potential fixes. We also release our code at our website [33].

In summary, this work makes the following contributions:

- To the best our knowledge, we are the first to perform AD planning-specific semantic vulnerability discovery. We focus on semantic DoS vulnerabilities, which can damage the availability of AD services. We formulate the problem with a domain-specific vulnerability definition and a practical threat model that only allows adding seemingly benign physical objects to the driving environment.
- To systematically discover the vulnerability, we design PlanFuzz, a novel dynamic testing approach that addresses various problem-specific design challenges: (1) propose and identify PIs as the testing oracle, (2) design a novel PI-aware physical object generation to systematically enforce problem-specific input constraints; and (3) design a novel behavioral planning vulnerability distance metric to effectively guide the discovery.
- We evaluate PlanFuzz on 3 planning implementations from two practical open-source AD systems. We find that PlanFuzz can effectively discover DoS vulnerabilities in all 3 implementations without incurring false positives. In total, 9 previously-unknown semantic DoS vulnerabilities are discovered, which can all be exploited to either prevent the victim from reaching its destination or cause an emergency stop. We find all our main designs are necessary, as without each design, statistically significant drops in performance are generally observed.
- We further perform 3 vulnerability exploitation case studies using simulation. The results show that the discovered vulnerabilities can cause the AD vehicle to unnecessarily stop permanently or give up necessary driving decisions. We also discuss root causes and potential mitigations.

II. Background & Problem Definition

A. Behavioral Planning (BP) in AD Systems

AD planning. In high-level (e.g., Level-4 [1]) AD systems, *planning* is a critical module designed to generate safe, efficient, and smooth driving trajectories to reach the destination. In industry-grade AD, such a module typically adopt a 3-layer design: *route planning*, *behavioral planning* (*BP*), and *local planning* [29, 30, 34–40]. Given the destination, *route planning* selects a route from the map. To follow the selected route while ensuring safety and correctness (e.g., conform to traffic rules), *BP* then makes high-level driving decisions such as cruising, stopping, lane changing, etc. based on the real-time driving environment. For example, when the AD vehicle needs to pass a signaled intersection, the BP layer needs to consider both the traffic light and the dynamic behaviors of surrounding vehicles and pedestrians to decide whether and when to proceed. Next,

local planning translates the high-level decisions into concrete low-level driving trajectories (e.g., waypoints), which will then be passed to the vehicle control module to actuate.

Our focus: AD Behavior Planning (BP). As described above, BP is at the core of AD decision making, and thus highly security/safety critical: any mistakes made in it can directly lead to undesired driving behaviors such as driving too *aggressively*, which can cause collisions, or too *conservatively*, which can cause unnecessary emergency stops and road blocking. In BP, the decisions can be generated from *programmed* or *learned* logic. There are some recent works exploring learning-based planning [41–43], but so far they are all experimental (e.g., designed and evaluated only for simulated racing game setups [44–48]) and generally lack the necessary capability and support for real-world driving (e.g., limited to only cruising without handling intersections, cross-walks, pedestrians [48–51], and no consideration of traffic rules [51–56]). Such a learning-based approach is also generally known to suffer from difficulties with debugging and interpreting [57], and enforcing safety rules/measures [58], while the latter is especially critical for production AD. Thus, the BP in today's industry-grade AD systems generally adopts programmed logic [29, 30, 59, 60]. Such program-based BP is thus also the main target of our design, which raises design challenges as detailed in §III-B.

B. Attack Goal and Incentives

Attack goal: Semantic Denial-of-Service (DoS) of BP. In this paper, we target an attack goal of causing *semantic Denial-of-Service (DoS)* on BP, which we define as causing it to change a normal driving decision to an *overly-conservative* one so that the victim AD vehicle will have a *failed* or *significantly-degraded* mission performance (e.g., never reach the destination). Specifically, we focus on 2 concrete types of such DoS in an AD context: (1) causing an emergency/permanent stop, and (2) causing the victim to give up a mission-critical driving decision, such as necessary left/right turns and lane changing on the route. To achieve this goal, in this paper we target *physical-world attack vectors* in the AD context (e.g., adding seemingly-benign static/dynamic physical road objects, detailed in §II-C) for high practicality and realism.

We choose to focus on causing overly-conservative driving decisions instead of overly-aggressive ones because we hypothesize that real-world BP, especially those in production settings, will *generally try to be as conservative as possible by design to avoid any possible safety incidents*. This is based on the fact that one single fatal crash (e.g., the Uber one [11] and increasingly more Tesla ones [12–14]), no matter whether it is mainly due to AD system flaws or not, can cause great reputational damage, lawsuits, and business being paused or even sold [61, 62]. In fact, such overly-conservative behaviors have *already been observed in real-world production AD*, causing troubles to AD service and traffic flows. For example, there is a video showing the AD vehicle from Waymo, a world-leading AD company, getting stuck by non-road-blocking traffic cones for $>$10 mins [17], in the parking lot when no other moving objects are around [15], and at an intersection resulting in blocking normal traffic [16]. A snapshot is in Fig. 1; since the environmental perception results are all correct according to the in-vehicle display [17], it is highly likely caused by planning flaws/bugs. There are more issues in the same vein reported for Waymo, Volvo, Uber, etc. [18–20].

Figure 1: Real-world overly-conservative driving behavior observed for a Waymo AD vehicle, which got stuck in the middle of the road and force other vehicles to borrow the reverse lane [17].

Problem seriousness and incentives. With the growing deployment of commercial AD services without safety drivers (e.g., by Waymo, Nuro, and Baidu [63–65]), such DoS problems can severely damage the availability of these services and thus ruin their user experience, reputation, and also revenues. It can help if remote operators are available, but such helps are not necessarily effective. For example, in the Waymo video above (Fig. 1), the AD vehicle called remote-operator help twice but it actually made the problem worse, and eventually called road assistance team to physically arrive, causing >10min trip delay in total. Such semantic DoS may also cause safety problems, e.g., by triggering emergency brakes in dangerous road segments like highway exit ramps, or blocking the road and thus forcing other vehicles to borrow the reverse lane like in Fig. 1. Since such consequences can at least damage the reputation of the victim AD company, one potential attack incentive is for business competition (e.g., by a rival AD company to unfairly gain competitive advantages).

Distinction to traditional software bugs. As illustrated in Fig. 2, the semantic BP DoS vulnerability targeted in this paper is a type of semantic software vulnerability for BP, which can be caused by either software design flaws or implementation bugs. The key distinction of such semantic vulnerabilities to traditional software bugs is that their symptoms are erroneous behaviors at the BP decision logic level (e.g., keep driving or not, change lane or not) instead of at the generic computer program level (e.g., software crash, memory corruption, hang). In our problem setting, since we target physical-world attack vectors (§II-C), the semantic BP vulnerabilities we target further differ in that the vulnerability triggering is via physical-world realizable perturbations (e.g., by adding attacker-controllable road objects) instead of generic program input changes (e.g., bit-level value changes of BP inputs), which is also illustrated in Fig. 2.

C. Threat Model

Attack vector: Attacker-controllable common physical-world road objects. Fig. 2 illustrates our threat model with a comparison to traditional software vulnerability exploitation. Instead of directly sending malicious inputs to the program, we assume that the attacker can only exploit semantic BP DoS vulnerabilities via *introducing common and easily-controllable*

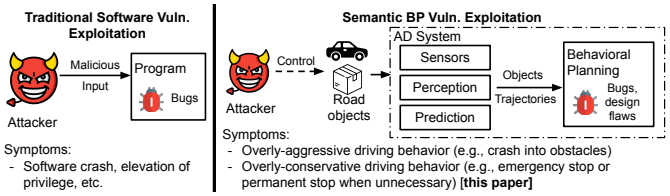

Figure 2: Illustration of the domain-specific threat model and exploitation symptoms of the semantic BP DoS vulnerabilities targeted in this paper, along with their distinctions to those of traditional software vulnerabilities.

external physical-world objects to the driving environment, e.g., dumped cardboard boxes, parked bikes on the road side, vehicles driving on the roadway, or pedestrians walking on road pavements. We choose such a threat model because the attacker can more realistically launch such an attack in a practical setting since the attacker does not need to compromise or tamper with the internals of the victim AD system and the objects can pretend to be benign once they follow basic traffic laws and driving norms. In §VII-B, we also discuss the capabilities of a stronger threat model that might also be able to compromise the perceptional sensors. Since this work aims at developing a systematic BP vulnerability discovery system for AD system developers, our system design assumes white-box access to the BP implementation.

Distinction to safety problems. Under such a physical-world attack threat model, the attack-targeted unintended BP decision behaviors are also possible to naturally occur in non-adversarial settings, making them also in the scope of general safety or robustness problems. Here, the distinction is that we focus on the set of such unintended behaviors that are *(more) triggerable* by attackers in the driving environment, e.g., easily-controllable road objects such as cardboard boxes, bikes, and attacker-driven vehicles, instead of weather conditions and road-side building locations/shapes. Such a security focus makes the discovered vulnerabilities arguably more severe, since with an adversary such unintended behaviors can be more frequently, controllably, and strategically triggered to cause more severe real-world consequences, e.g., causing emergency brakes in more dangerous road segments such as highway ramps, and causing traffic blocking in mission-critical roads such as in front of police stations or fire stations.

III. Motivation and Challenges

In this section, we use a motivating example to concretely describe the BP DoS vulnerabilities targeted in this paper and the design challenges to systematically discover them.

A. Motivating Example

Fig. 3 shows the simplified pseudo code for a BP DoS vulnerability our system discovered from version 5.0 of Apollo, an open-source industry-grade AD system [29] (also confirmed that such vulnerability also exist in 6.0, the latest version). This logic is from `path_bounds_decider`, one of the BP decision-making steps for the lane following scenario that checks whether the current lane has enough space in the lateral

```
1  # Pre-defined lateral safety buffer, in meter
2  obstacle_lat_buffer ← 0.4f
3  ADC_width ← 2.11f #Default AD veh width,in meter
4  #Initialize left/right boundaries of drivable
   ↪  space
5  {left_bound, right_bound} ← {left_lane_boundary,
   ↪  right_lane_boundary}
6  # Iterate over static obstacles at this
   ↪  longitudinal position
7  for (each obs in obstacles_list)
8    if ((obs.min_l+obs.max_l)/2<0): # Left-side
     ↪  obstacles
9      left_bound ← max(left_bound, obs.max_l +
       ↪  obstacle_lat_buffer)
10   else: # Right-side obstacles
11     right_bound ← min(right_bound, obs.min_l -
       ↪  obstacle_lat_buffer)
12 # Check whether exists drivable space laterally
13 if (right_bound - left_bound < ADC_width):
14   path_blocked ← true #Conclude: lane is blocked
```

Figure 3: Simplified pseudo code for a semantic DoS vulnerability PlanFuzz discovered from BP in Apollo, an industry-grade AD system [29].

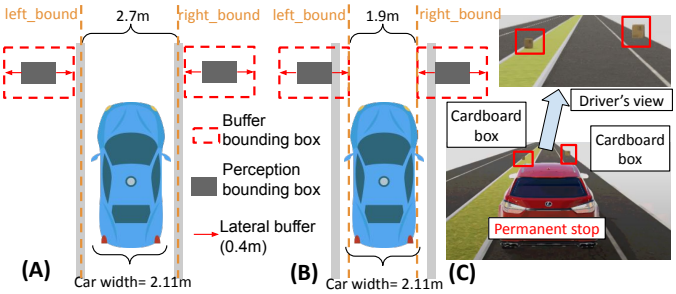

Figure 4: Illustration of (A) BP decision logic in Fig. 3; (B) its semantic BP DoS vulnerability; (C) potential real-world exploitation of it from our end-to-end simulation case study (§VI).

direction (left/right) for the AD vehicle to drive; if not, it considers the lane as blocked.

Decision logic. As shown in Fig. 3 and illustrated in Fig. 4 (A), this code maintains 2 variables, `left_bound` and `right_bound`, to represent the leftmost and rightmost boundaries of the drivable space for a given longitudinal (forward/backward) position. If the space between these two boundaries is smaller than the AD vehicle width `ADC_width` (line 13), it means no drivable space laterally and thus the current lane is blocked. The two variables are initialized with the left and right lane boundaries (line 5). Next, it iterates over the list of detected surrounding static obstacles, and use the rightmost lateral boundaries (`obs.max_l`) of the left-side obstacles to update `left_bound` (line 8-9), and the leftmost lateral boundaries (`obs.min_l`) of the right-side obstacles to update `right_bound` (line 10-11). Such logic can thus avoid causing the vehicle body to hit/touch the static obstacles. Here, a lateral *obstacle safety buffer* (`obstacle_lat_buffer`, line 2) is conservatively applied to the leftmost and rightmost boundary calculation (line 9, 11) on top of the detected obstacle boundaries from the perception module, to ensure that the vehicle can keep enough distance from the obstacles.

BP DoS vulnerability. In Apollo 5.0, the obstacle safety buffer above is set to a constant value, 0.4m, regardless of obstacle positions in the driving environment. Meanwhile, the minimal lane width is 2.7m in urban areas [66], and thus

static obstacles out of the boundaries of such lanes can in the extreme case reduce the lateral drivable space between `left_bound` and `right_bound` to 1.9m ($2.7 - 0.4 \times 2$). This is actually narrower than most vehicle models popularly used for AD today, e.g., 2.11-2.14m (with mirrors) for Lincoln MKZ, Lexus RX, Jaguar I-Pace, etc. [67–70]. As shown in Fig. 3, the default value in Apollo is set to 2.11m (line 3). This means that with such logic a lane can be considered as blocked *even when its designed drivable space is completely empty with no static obstacles invading its lane boundaries*. For a single-lane road, this means that the whole road is considered blocked and thus the AD vehicle will *permanently* stop at the current lane, as illustrated in Fig. 4 (B). This is a decision flaw for BP as such driving behavior is *too conservative* to the extent that it *directly* violates common driving norms. For example, the requirement that a vehicle "should never block the normal and reasonable movement of traffic" [71], which can result in the vehicle being cited if this requirement is violated, especially when such a violation occurs inside a tunnel or 15 ft within a fire station's driveway [72].

Based on the code logic, the root cause for such an overly-conservative BP decision flaw is in the use and setting of the obstacle safety buffer. We found that such a flaw is not specific to Apollo: our system discovers that Autoware, another popular open-source full-stack AD system [30], has similar flawed BP logic even though the concrete implementation is quite different from Apollo's. Also, Autoware is even more conservative in such buffer settings (§V-B). This thus conforms to our general design hypothesis in §II-B that BP for practical AD systems tends to be as conservative as possible, leading to a general susceptibility to semantic DoS vulnerabilities.

Exploitation. To exploit this vulnerability in the real world, an attacker simply needs to prepare 2 easy-to-carry static objects that are not too uncommon in road regions, e.g., cardboard boxes, and place them close to but still off the lane boundaries on each side of a single-lane road, as illustrated in Fig. 4 (B). This is seemingly benign as these boxes are not blocking road and such randomly-dumped garbage on road side is not entirely uncommon. However, it can cause the AD vehicle with the vulnerable BP logic above to get permanently stuck at this road position and block traffic. Note that these 2 boxes do not have to be at exactly the same longitudinal position; from the code, they can be up to 5m (in the latest Apollo version) apart in longitudinal direction while still causing such a permanent stop decision, which can make such exploitation look more benign and thus stealthier. We did not include such longitudinal direction logic in Fig. 3 for the ease to understand the key vulnerable logic. Fig. 4 (C) shows a snapshot of our end-to-end simulation case study of this exploit for Autoware (detailed in §VI). As shown, the two boxes are clearly off road and far from blocking the road, but the AD vehicle is forced to permanently stop there.

B. Design Challenges

Motivated by the concrete example above and similar problems observed in real-world production AD settings today (§II-B), it is highly desired to develop a systematic approach to discover such BP DoS vulnerabilities at the AD system development stage so that the developers can proactively find and fix them before deployment.

Recently, property-based testing have achieved great success in discovering safety violations in AD software [10, 28, 73–77]. We follow the same general framework to develop a tool which can systematically discover DoS vulnerabilities in AD software. In the motivating example, the property we aim to falsify can be formally expressed as:

$$IsSafetoDrive \rightarrow \neg Stop \tag{1}$$

The above property indicates that when the current lane is safe to drive, the vehicle should be able to normally follow the lane instead of getting stuck by irrelevant physical objects. Even though the property seems to be simple at the first glance, none of previous works can be directly applied to solve this problem due to the following design challenges:

C1. Lack of testing oracles for semantic DoS vulnerability in BP. For our vulnerability definition (§II-B), a key challenge is how to judge whether the current situation is safe to perform a certain planning behavior. For example, in our motivating example in §III-A, we need to decide the value of predicate *IsSafetoDrive* in Eq. 1. Previous works [10, 28, 73–75] focus on the safety properties, especially collision, which can be directly extracted from official documentations or easy to define. But when it comes to studying DoS properties, there is no clear boundary of whether it is safe for the vehicle to drive due to the uncertainty and complexity of the environment. The first challenge is that we need to *concretize* the predicate *IsSafetoDrive* in Eq. 1 into expressions which can be directly computed from planning inputs.

C2. Need to systematically generate attack inputs following complicated problem-specific physical constraints. To discover our BP DoS vulnerability, the dynamic testing process needs to effectively generate attacker-introduced physical-object properties (e.g., positions) that can (1) follow basic traffic rules and driving norms as required in §II-C to achieve high attack practicality and stealthiness, e.g., a moving attack vehicle should drive in a lane following the road direction, instead of on pavements or in the wrong direction; and (2) make sure the value of predicate *IsSafetoDrive* is true, since we can only find counterexamples when this predicate is true. Both constraints require to resolve complicated problem-specific geometry constraints; the closest solution so far is from Scenic [78], which can generate test inputs within several generic geometric constraints in AD context (e.g., certain distances of a road object to curb). However, it still cannot address the more complicated ones specific to our problem context. For example, since we specifically want to generate road objects that should not affect the ego vehicle driving decision, their geometry constraints are inherently dependent on the planned trajectory of the ego vehicle, e.g., cannot be on or have any intention to move to any lanes that the ego vehicle plans to drive on (PI-C1, C4, C5 in Table I). However, Scenic's current design does not consider such dependencies.

C3. Need to obtain more fine-grained feedback from the planning decision-making code level (i.e., decision code branches) to guide our vulnerability discovery. For automated software vulnerability discovery in general, existing dynamic testing methods popularly obtain code-level feedback to guide the discovery process, which shows superior effectiveness over treating the software as a black-box [79–83]. In the general CPS testing domain, prior works have used quantitative feedback such as the robustness metrics to guide testing [28, 76], but such a guidance still treats the code-level decision logic (i.e., decision-making code branches) as black-box, which thus cannot provide guidance once the overall planning output stays unchanged. In our problem setting, it is desired if we can improve this with more fine-grained code-level guidance such as the distance between the current inputs and the planning decision boundary at the code branch level. For example, in Fig. 3, the guidance can be more effective if we can leverage the value distance between `left_bound` and `right_bound` at the decision code branch at line 13.

IV. Design: PlanFuzz

In this paper, we are the first to address the 3 challenges in §III-B by designing an automated approach to systematically discover BP DoS vulnerabilities (§II-B), called *PlanFuzz*.

Design goal. The goal of PlanFuzz is to discover previously-unknown semantic DoS vulnerabilities defined at the BP decision code level (an example is in §III-A). Note that our current focus is not on the comprehensive identification of the triggering scenarios for the discovered vulnerabilities; nevertheless, a few concrete triggering scenarios will come with the discovery to provide the vulnerability triggerability since we adopt a dynamic testing framework (detailed below).

A. Overview of Key Designs

At a high level, PlanFuzz follows an evolutionary testing framework, which is widely adopted by prior works on domain-specific vulnerability discovery with high generality, effectiveness, and efficiency [21, 26, 84–86]. To address the challenges in §III-B, the following key designs are introduced:

Planning Invariant (PI) as testing oracle. To address $C1$, we propose *Planning Invariant (PI)* as the problem-specific testing oracle for BP DoS vulnerabilities. PI has 3 components: *planning scenario*, *constraints for physical objects*, and *desired planning behavior*, which together define an invariant property for BP: In a planning scenario, the BP output should always conform to the desired planning behavior as long as the PI constraints for surrounding physical objects are satisfied. For example, for our motivating example in §III-A, the planning scenario is lane following; the PI constraints for physical objects are that the surrounding physical objects are all static and located outside the lane boundaries; the desired planning behavior is that the AD vehicle should keep driving forward. Such invariant properties are derived from common driving norms (e.g., off-road static obstacles should not be considered as blocking the road, detailed in §IV-C) so that its violations can be used to tell an overly-conservative decision.

PI-aware physical-object generation. To address $C2$, we need to design physical-object generation methods that conform to both the driving norms (e.g., traffic rules) and PI constraints above given a planning scenario and desired planning behavior. A direct solution direction is to directly generate random physical-object properties within these constraints. However, generating them following a random distribution is very difficult since these constraints are quite irregular in the real world (e.g., curvy and zigzag road boundaries), not to mention the problem-specific constraints due to the dependence on the planned trajectory of the ego vehicle (§III-B). To address this, our strategy is to first generate objects without considering these constraints, and then add a PI constraint enforcement step afterwards to adjust its properties (e.g., positions) for conformation. Specifically, here different PI constraint enforcement operators are designed following the diversity and inheritance principles desired for the random input generation step in genetic algorithms [87].

BP vulnerability distance. To overcome $C3$, we design *BP vulnerability distance* as the code-level feedback to measure how close the current BP execution is to violate a PI and thus trigger a BP DoS vulnerability. Specifically, such a distance is defined based on the control- and data-flow differences between the current executed code path and its closet path to a set of *attack target positions*, which are code positions indicating violations of the PI (for example, the callsite of API *BuildStopDecision*). To facilitate its run-time calculation during the dynamic testing, we first perform an off-line analysis of the BP code to (1) identify the key predicates that the attack target positions control- and data-dependent on, and compute information that can be pre-calculated about their run-time control- and data-flow distances to the target positions, which forms a *BP vulnerability distance profile*; and (2) instrument these predicates to collect their execution status, called *BP vulnerability trace*, in the run time. During the testing, based on the execution status of these key predicates collected in BP vulnerability trace, the control- and data-flow distances of the executed key predicates are calculated with the pre-computed information from BP vulnerability distance profile, which are then combined to calculate the final vulnerability distance.

Next, we describe the whole PlanFuzz system design incorporating these key designs, and then provide details for each.

B. PlanFuzz System Design

System input and output. Fig. 5 shows an overview of PlanFuzz system with the key designs above. As shown, the whole PlanFuzz system requires 3 inputs: (1) BP source code (we assume it is avaiable since PlanFuzz is designed for AD developers); (2) BP input traces (including map) for the planning scenarios of interest; and (3) a set of PIs for these scenarios. The output is a set of test inputs that can trigger a BP DoS vulnerability. The AD developers can then utilize them to identify the vulnerable code logic and analyze root causes, with the goal of developing vulnerability fixes.

Manual efforts. Three types of manual efforts are required for using PlanFuzz: (1) Collecting BP input traces for the

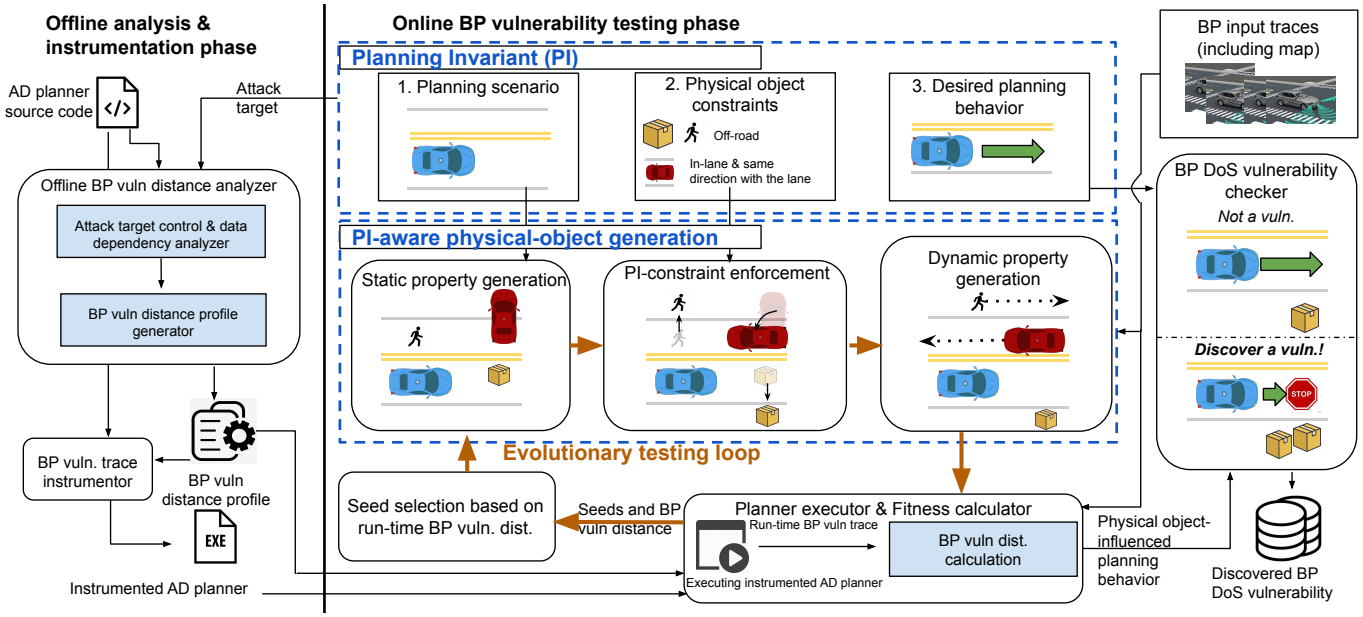

Figure 5: Overview of PlanFuzz, our automated approach for systematically discovering BP DoS vulnerabilities in AD systems.

targeted scenarios. Since PlanFuzz is designed for AD developers, we assume they have access to such traces from their AD system testing or operations; (2) identifying PIs for these targeted scenarios. Note that such identification is an one-time effort and there are general ones applicable across multiple scenarios identified later in §IV; and (3) identifying and annotating the attack target positions in the source code. For AD developers, we assume they can have high-level knowledge of the BP code (e.g., BP decision APIs and state variable class) to identify these based on the desired planning behavior of PI and the state variables associated with the scenarios. In our experiments, it took less than 50 lines in total and less than 1 hour of manual efforts for an author who is experienced with the AD planning code.

System framework. With the inputs above, the vulnerability discovery process has 2 phases as shown in Fig. 5: (1) *offline analysis and instrumentation*, and (2) *online BP vulnerability testing*. On the left side of Fig. 5, the offline phase takes the BP source code and attack target positions based on PIs, and generate the BP vulnerability profile and instrumented BP code. On the right side of Fig. 5, the online phase follows the evolutionary testing framework in which each single physical object is considered as a "gene". It customizes each component of a genetic algorithm: (1) *fitness*, for which we use the run-time BP vulnerability distance to measure how close a BP execution is to trigger a BP DoS vulnerability. It is calculated by executing the instrumented BP code in the planner executor and the fitness calculator in Fig. 5; (2) *mutation and crossover*, for which we use the PI-aware physical-object generation to mutate and exchange physical objects; (3) *seed selection*, for which we select test cases with smaller BP vulnerability distances as the new seeds.

To get started, the planner executor extracts the input frames corresponding to each BP decision from the BP input trace, and then feeds these frames to the instrumented BP code.

Table I: General PI (Planning Invariant) constraints across different driving scenarios from the full list of PIs identified and used in this paper (Table IV).

Physical object type	PI constraints for physical objects
Static obstacle (cardboard boxes, parked bikes, etc.)	PI-C1. $StaticOffRoad(x)$
Vehicle	PI-C2. $IsFollowingVehicle(x)$ PI-C3. $IrrevalentVehicle(x)$
Pedestrian	PI-C4. $StaticOffRoad(x)$ PI-C5. $DynamicOffRoad(x)$

To maintain the consistency of internal BP states, we record a snapshot of the internal state variables beforehand for the initial seed, and recover it before feeding the testing inputs later. During the testing, the BP DoS vulnerability checker determines whether a certain generated testing case violates the PI; if so, it outputs the discovered vulnerability.

C. Planning Invariant

As introduced in §IV-A and shown in Fig. 5, each PI has 3 components: planning scenario, constraints for physical objects, and desired planning behavior, which together form the BP invariant properties that concretely define the overly-conservative BP decisions. In this paper, we consider 8 different planning scenarios commonly supported by industry-grade AD systems [29, 30, 88], covering various basic real-world driving scenarios, e.g., lane following, lane changing, intersections with stop signs and traffic signals, lane borrowing, bare intersection, and parking. The full list is in Table IV. Since we target semantic DoS vulnerabilities, the desired planning behavior for each scenario is usually to just keep the intended driving behavior, e.g., keep cruising for lane following, keep moving to pass the intersection, and finish the lane-change/borrow/parking actions.

Given a planning scenario and the desired driving behavior, the next is to identify the physical-world constraints of the attacker-introduced physical objects such that if satisfied, the BP logic should not give up the desired driving

behavior. We derive such constraints conservatively based on common driving norms, e.g., descriptions from the driver's handbook [71] such as those quoted in §III-A. Specifically, in this paper we focus on the general constraints that are applicable to multiple driving scenarios, which are summarized in Table I and denoted as *PI-C*. For example, for static obstacles such as cardboard boxes and parked bikes, the ones that are completely off-road and without any violation of the boundaries of the lanes, which the AD vehicle plans to drive on, should generally not cause the BP logic to give up lane following, changing, borrowing, or passing an intersection. For pedestrians and vehicles, the ones moving in their commonly-designated regions (e.g., off-road pavement for pedestrians, and traffic lanes for vehicles) without showing any intention to move towards the AD vehicle or the lane regions the AD vehicles plans to drive one should not give up those desired driving decisions. Here for the simplicity, we define a list of functions $StaticOffRoad(x), DynamicOffroad(x), FollowVehicle(x), IrrevalentVehicle(x)$ to express the geometry relationship between the road network, the trajectory of a certain physical object x, and the trajectory of the AD vehicle. The complete set of PI-Cs for all planning scenarios and the formal definitions of the functions are in Table IV in Appendix. With the defined PI-Cs, we are able to concretize the high-level property in Eq 1 into the following format to describe the property in lane following scenario:

$$\begin{aligned} StaticCons(x) &:= (x.type == Static) \rightarrow (StaticOffRoad(x)) \\ VehicleCons(x) &:= (x.type == Vehicle) \rightarrow \\ &\quad (FollowVehicle(x) \vee IrrelevantVehicle(x) \\ PedestrianCons(x) &:= (x.type == Pedestrian) \rightarrow \\ &\quad (DynamicOffroad(x) \vee StaticOffRoad(x)) \\ &\wedge_{x \in O}((StaticCons(x)) \wedge (VehicleCons(x)) \\ &\quad \wedge (PedestrianCons(x)) \rightarrow \neg Stop \end{aligned} \tag{2}$$

Here O is the set of physical objects and x is a physical object in the set. We define the constraints for each type of objects and merge them in the end to define the availability property.

D. PI-aware Physical-Object Generation

After concreting the property, the next step is to generate the inputs that can always satisfy the constraints in planning invariant. In other words, we want to make sure that the left side of Eq. 1 is always true. We design PI-aware physical object generation to satisfy this requirement. Due to the page limit, we leave most of the details in our extended version [89]. The input generation contains three main steps:

Static property initialization and mutation. In this step, we first randomly generate the static properties of the objects, e.g., position, type, and size, without considering PI-Cs during the testing input initialization and mutation processes. For each generated physical object, we will assign an appropriate size given the randomly generated object type.

PI-constraints enforcement. The second step is to change the position and heading of each physical object to enforce the position correctness for each object. The high-level idea

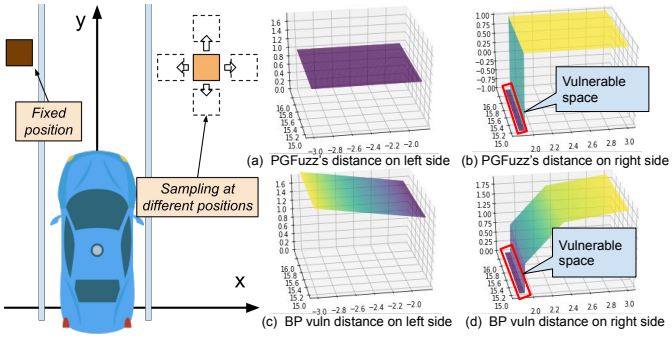

Figure 6: Illustration of the benefit of our BP vulnerability distance design compared to other fitness function choices.

of this enforcement step is to adjust the property value to the closest one that does not violate PI-C. For example, moving a static obstacle, which violates the lane boundaries, to the closest off-lane position. We also change the lateral position and longitudinal position separately to keep the diversity and inheritance during the evolutionary algorithm.

Dynamic property generation. The last step is to add dynamic properties (e.g., speed and moving trajectory) for dynamic physical objects such as driving vehicles and walking pedestrians. Here, the generated properties need to ensure (1) satisfying the driving norms (e.g., traffic rules) as in §II-C, and (2) conforming to the related PI-Cs such as not showing any intention to move towards the AD vehicle or the lanes it plans to drive on (PI-C3,5 in Table I).

E. BP Vulnerability Distance

The BP vulnerability distance is calculated based on information from both offline BP vulnerability distance profile and runtime BP vulnerability trace. If we recall the example code in Fig. 3, our goal here is to find a set of physical objects, which satisfy the constraints of PI, and make the program execution reach line 14. Inspired by directed greybox fuzzing [90], we design a distance metric to quantify the distance between current execution trace and the attack target positions. The directed greybox fuzzing techniques so far generally only consider control flow distance defined in [90]. In this paper, we further add a data flow distance into our distance metric design. This is motivated by our observation: (1) The BP decision-making is usually based on a list of predicates with floating-point number comparisons. Thus, measuring the difference between floating points operands can help guide the testing in a more fine-grained way. (2) The control-flow changes in our problem setting is not very significant. For example, in the path bounds case shown in §III-A, changing the position of a certain obstacle will not change the overall control flow unless a different decision is made.

Specifically, in the offline analysis and instrumentation phase as shown in Fig. 5, we first build a Program Dependence Graph (PDG) of the BP code and then use it to identify all the predicates that the attack target positions control- and data-dependent on. We further divide the predicates into two parts: critical predicates and non-critical predicates. Critical predicates refer to the predicates that connect themselves with

the attack target position with control dependence edges only. On the other side, non-critical predicates refer to the predicates that must connect with the attack target via data dependence edges. Examples for these two types of predicates based on our motivating example are included in our extended version [89].

For each of these predicates, we calculate their individual control- and data-flow distances, and use the sum as the overall BP vulnerability distance. Our control-flow distance design is similar to that in prior directed grey-box fuzzing methods [90], and thus next we focus on explaining our data-flow distance design using run-time collected BP vulnerability traces. For critical predicates, our offline phase determines which branch is reachable or closer to the target positions. In the runtime, we calculate how close the execution is to triggering such a branch using the differences between the operands and the execution number of each branch. For non-critical predicates, since we do not know which branch is the closer branch towards the target positions, our strategy is to minimize the difference between operands to get more diverse execution traces.

We use the motivating example in §III-A to demonstrate the benefit of this design. As illustrated in Fig. 6, we fix the position of one static object right next to the left lane line and 15m in front of the AD vehicle, and at the same time, we arbitrarily move the other static object and measure the robustness distance metric used in [28, 76, 77] and BP vulnerability distance proposed by our paper. In Fig. 6 (a)(b), the robustness metric can only give a boolean guidance on whether the decision is changed. However, our distance metric in Fig. 6 (c)(d) can guide the position of the second object into the vulnerable area due to that the operand distance of predicate on Line 8 and Line 13 in Fig. 3 becomes smaller when the object is approaching to the vulnerable area.

V. Evaluation

A. Evaluation Setup

Subject BP implementations. We evaluate PlanFuzz on the BP code from 2 open-source AD systems, Baidu Apollo [29] and Autoware [30]. Both are practical full-stack AD systems that can be readily installed on real vehicles for driving on public roads [91, 92], and also have representativeness for industry-grade AD systems as Baidu has been recently ranked among the top 4 leading industrial AD developers with Waymo, Ford, and Cruise [31] and has been providing self-driving taxi services in China for months, while Autoware is adopted by the USDOT in their AD vehicle fleet [32].

Specifically, we select the BP implementations in 2 Apollo versions, 3.0 and 5.0, as their design and implementations are significantly different based on the release log [93]. We did not evaluate on 6.0, the latest Apollo version, as it only made minor changes to 5.0 in BP [93]. We have confirmed that all the discovered vulnerabilities from 5.0 also exist in 6.0. The Autoware BP implementation we evaluate on is from Autoware.AI 1.14.0 [30, 94], the latest version with an implementation of the open planner [95]. Both Autoware and Apollo use rule-based logic to make decisions. Their main difference is that Autoware's BP adopts a single finite state machine-based design where all planning behavior changes are modeled as state transitions, while Apollo's is more modular, which first decomposes the whole driving decision making into independent primitive tasks (e.g., obstacle avoidance, lane changing, intersection passing, velocity selection, etc.) and then selects the appropriate ones based on different driving scenarios (e.g., lane following, intersection, stop sign).

BP input trace collection. We use LGSVL, a production-grade AD simulator [96], to collect the BP input traces as the initial testing seed (§IV-B). The benefit of using a simulator to generate seeds is that it is easier to (1) create different planning scenarios to increase testing diversity, and (2) control the scenario to prevent any irrelevant physical objects from affecting the generation of desired planning behavior. Note that such simulation-based testing is widely used in the AD industry for flexibility, scenario coverage, and safety [97–99]. LGSVL itself is also designed for performance and safety testing of production AD systems [96].

In total, 40 traces are collected under 8 different driving scenarios (5 per scenario). For each scenario, the 5 traces have diversity in driving tasks (e.g., drive straight or make turns) and road layouts (e.g., width of the local road's lane width or the highway). Each trace spans up to 47sec with 100-2400 BP decisions, and the input frame for each BP decision is used as an individual testing seed. These traces lead to 28,789 (9,676 for Apollo, 19,113 for Autoware) different initial testing seeds in total (3,598 per scenario on average) used in our evaluation. Details are in our extended version [89]. In these traces, both the AD vehicle itself and other traffic participants are behaving normally/correctly (e.g., follow traffic rules and driving norms, and can correctly execute the designed driving maneuvers).

Test input generation. For each initial testing seed, PlanFuzz generates the attack's physical objects as described in §IV-D and injects them into the planning input. Here, we directly use their ground-truth physical properties (e.g., type, bounding-box size and shape), which can thus avoid finding violation cases due to errors in upstream modules (e.g., perception) instead of BP. As described in §IV-D, for each attack object, PlanFuzz initializes and mutates their properties within common feasible ranges according to their types. For example, the positions of generated objects is within 80m to the ego vehicle (a common range of AD perception [100]); the sizes for static objects are 0.5-2m each dimension, and those for pedestrians and vehicles are the same as the default ones used in the simulator. Details are in our extended version [89]. Note that consistent with our threat model (§II-C), we do not mutate the non-attacker-controllable planning inputs such as weather conditions and the ego vehicle's driving speed; all of them just inherit the valid values from original BP input traces.

Evaluation metrics and setup. We consider a vulnerability as discovered when any attack target position is triggered (§IV-B). We consider a discovered BP DoS vulnerability *unique* if its code-level decision logic (branches) that causes such vulnerability (e.g., those in §III-A) is different from the others, which is similar to unique crashes in traditional fuzzers [101–104]). For each initial seed, we run PlanFuzz

Table II: Discovered BP DoS vulnerabilities from Apollo (3.0, 5.0) and Autoware. PI identifiers refer to PIs in Table IV in Appendix. All the vulnerabilities discovered in Apollo 5.0 are confirmed to also exist in the latest version Apollo 6.0.

Vuln #	Driving Scenario	Software	Violated PI #	Attack-influenced Planning Behavior	Triggering Objects
V1	Lane following	Apollo 3.0/5.0	PI1 (PI-C1)	Permanent stop	Static obstacle
V2	Lane changing	Apollo 3.0/5.0	PI3 (PI-C2, 3)	Fail to change lane and never reach destination	Vehicle
V3	Lane borrow	Apollo 3.0/5.0	PI4 (SP-PI-C1, 2)	Fail to borrow the lane and permanent stop	Vehicle or static obstacles in front of blocking vehicle
V4	Lane borrow	Apollo 3.0/5.0	PI4 (PI-C1, 4, 5)	Fail to borrow the lane and permanent stop	Off-road static obstacle
V5	Intersection w/ traffic signal	Apollo 3.0/5.0	PI6 (PI-C4)	Fail to pass intersection and permanent stop	Static pedestrian
V6	Intersection w/ traffic signal	Apollo 3.0/5.0	PI6 (PI-C5)	Emergency stop; possible to cause permanent stop and thus fail to pass intersection	Pedestrian who is leaving the intersection
V7	Intersection w/ stop sign	Apollo 3.0/5.0	PI5 (PI-C1)	Fail to pass intersection and permanent stop	Static bicycle off the road
V8	Lane following	Autoware	PI1 (PI-C1)	Permanent stop	Static obstacle off the lane
V9	Lane following	Autoware	PI1 (PI-C3)	Emergency stop	Moving vehicle off the lane

multiple times to increase the chance of finding unique vulnerabilities. For each run, the testing terminates when either a vulnerability is found, or the optimal fitness value is unchanged for 100 generations. We manually verified each discovered vulnerability and did not find any false positives.

B. Vulnerability Discovery Effectiveness

Throughout our experiments, PlanFuzz discovered 9 unique BP DoS vulnerabilities in Apollo and Autoware as shown in Table II. All these vulnerabilities can be exploited to adversely delay the progress of the AD vehicle from reaching its destination; most of them can cause the AD vehicle to permanently stop on the road. We classify the vulnerabilities into three types based on the attack scenarios. In this section, we provide a summary of the attack scenarios, including (1) the driving scenarios and symptoms of the relevant vulnerabilities, (2) the violated PIs, (3) the root causes, and (4) the potential real-world exploitations. Pseudo code and detailed analysis of the vulnerabilities can be found in our extended version [89].

Attack scenario 1: Lane following DoS attack. In this scenario, the AD vehicle keeps cruising in the current lane while static or dynamic obstacles located outside of the current lane boundaries. Leveraging V1/V8/V9, the attacker can cause the AD vehicle to decelerate or permanently stop in the current lane, which effectively prevents the AD vehicle from reaching the destination. Here, since the designed drivable space (i.e., the current lane) is completely empty with no obstacles invading the lane boundaries, such BP decisions thus violate PI1 or PI2 depending on the road structure (i.e., single- or multiple-lane road). As discussed in §III-A, the root cause is the setting and usage of the lateral obstacle safety buffer, which leads to the overly-conservative BP decisions.

To exploit V1 or V8, the attacker needs to find a single-lane road (for V1, the lane width needs to match the corresponding requirement described in §III-A) and place static obstacles close to the lane boundaries. The AD vehicle will then permanently stop in front of the static obstacles. To exploit V9, multiple attackers can coordinate to drive two vehicles in front of the AD vehicle on the lanes other than AD vehicle's current lane to trigger a deceleration decision.

Attack scenario 2: Intersection passing DoS attack. The third type of attack happens when the AD vehicle is approaching an intersection. V5–7 belong to this type and enable the attacker to cause the AD vehicle to stop in front of the crosswalk or even permanently stop before the stop sign. Since the static objects are all off-road and the dynamic objects' movement will not affect AD vehicle's planning behavior, the stopping decisions produced by BP thus violate PI5 and PI6. When passing the crosswalk, the AD vehicle needs to make sure there is no pedestrian inside the crosswalk or with the intention to move into the crosswalk. However, due to the overly-conservative distance checking between the AD vehicle's driving path and a standing pedestrian (V5) or trajectory collision checking between AD vehicle and a moving pedestrian (V6), the BP decides to stop before the crosswalk despite its driving path is in fact clear. For the intersection with stop signs, the BP maintains a watch list for the objects that arrive earlier such that it can proceed following a first-come first-serve convention. However, due to the overly-conservative distance threshold to the closest lanes when considering which objects it should wait for, the BP mistakenly includes parked bikes off the road into the watch list. Since these bikes are static, the AD vehicle keeps waiting for them and thus permanently stops before the stop line.

By exploiting V5 and V7, the attacker can cause the AD vehicle to permanently stop at the intersection. To achieve that, the attacker only needs to have a standing pedestrian or parked bikes around the intersection. For V6, since the pedestrian must be moving and will eventually leave the intersection, the attacker can thus carefully control the movement of the pedestrian such that the AD vehicle continuously applies a large deceleration, which may pose safety threats to the passengers and other vehicles (§II-B).

Attack scenario 3: Lane-changing DoS attack. This type of attack happens when the AD vehicle is about to change lanes or borrow the reverse lane due to the routing requirement or a blocking static obstacle. By exploiting V2–4, the attacker is able to use non-blocking static obstacles or following vehicles to prevent the AD vehicle from performing the desired lane-changing or lane-borrowing behaviors. As the

changing and borrowing lanes are clear in such scenarios, the vulnerabilities thus make the BP violate PI3 and PI4 for the lane-changing and borrowing scenarios. Specifically, V2 is caused by overly-conservative design when checking if the AD vehicle's future driving path overlaps with other vehicles during the lane-changing. V3 is caused by wrong judgement on whether it is necessary to borrow the lane. Although PlanFuzz mainly aims to find BP DoS vulnerabilities introduced by overly-conservative planning decisions, V4 is likely due to an implementation bug when checking whether the perception range is blocked by any obstacle before performing lane borrowing. More details of the vulnerabilities are in our extended version [89].

The attacker can exploit V2 by driving a vehicle tailgating the AD vehicle in the same lane. As long as the attacker's vehicle is close to the left lane line (but without touching the lane line), the AD vehicle will mistakenly interpret that the changing lane is blocked and give up the lane-changing attempt, which in the worst case can cause significant delays for the AD vehicle to reach its destination if the attacker keeps performing such attack. To exploit V3 and V4, the attacker first needs to find a lane borrowing condition where the road is blocked by a static obstacle (e.g., a truck which is unloading the cargo). Second, the attacker can park another vehicle in front of the truck (V3) or simply place an off-road cardboard box 5m away from the AD vehicle (V4).

C. Baseline Comparison

Since there is no existing alternative fuzzer that directly performs BP DoS vulnerability discovery, we evaluate the benefits of our designs by replacing important design components in PlanFuzz with possible baseline designs. Specifically, through such an evaluation we aim at answering the following methodology-level research questions (RQ):

RQ1. Can our BP vulnerability distance design (§IV-E) provide effective guidance to benefit the vulnerability discovery?

RQ2. Can our PI-aware physical-object generation design (§IV-D) benefit the vulnerability discovery?

RQ3. Can traditional fuzzing techniques without using any of our problem-specific fuzzing designs also effectively discover BP DoS vulnerabilities?

Baseline setups. To answer RQ1, we create a baseline setup, *PlanFuzz*$^{-guide}$, that replaces the BP vulnerability distance-guided genetic algorithm with random sampling (while still using all other PlanFuzz components such as PI-aware physical-object generation). For RQ2, we create another baseline setup, *PlanFuzz*$^{-PI}$, that keeps the BP vulnerability distance design but remove the steps that enforce PI constraints in the generated attack objects' static and dynamic properties, which are the key problem-specific designs in PI-aware physical-object generation (§IV-D). For RQ3, we remove both BP vulnerability distance and PI-aware physical-object generation designs; we directly use Protobuf-mutator for the entire test input generation process (denoted as *PB-M*). Protobuf-mutator is a readily-available fuzzer designed specifically for the data structure of protobuffers [105], which is directly compatible with the BP input data structure in both Apollo and Autoware.

Evaluation setup and metrics. We use the initial testing seeds that allow PlanFuzz to discover the 9 vulnerabilities in Table II to perform this baseline evaluation. For each seed, we run each of the 4 setups (full PlanFuzz and the 3 baselines) for 10 times, each time for 24 hours, to avoid variance as suggested by prior work [106]. For each fuzzer setup, we measure the discovered unique vulnerabilities (defined in §V-A), and their average Time-to-Exposure (μTTE), i.e., the time taken to discover them. When comparing a given baseline setup with the full PlanFuzz, we also use statistical testing following the suggestions in [90, 106, 107]. Specifically, we use the *Vargha-Delaney statistic* $\hat{A}_{12}$ to measure the effect size, and use *Mann-Whitney U* [107] to measure the statistical significance of the μTTE performance drop (recommended for assessing randomized algorithms like fuzzers [90, 107]).

Results. As shown in the last column of Table III, PB-M, the setup without using any of our main problem-specific designs, fails to detect *any* of the 9 BP DoS vulnerabilities within 24h, which is thus at least $57\times$ less efficient/effective. This concretely shows that our two main problem-specific fuzzer designs, BP vulnerability distance (§IV-E) and PI-aware physical-object generation (§IV-D), are *necessary* for effectively discovering BP DoS vulnerabilities (RQ3).

For PlanFuzz$^{-\text{guide}}$ and PlanFuzz$^{-\text{PI}}$, the setups that each still retains one of these two problem-specific designs, the same set of unique vulnerabilities (as full PlanFuzz) are still discoverable within 24h. However, their discovery efficiency degrades substantially compared to the full PlanFuzz. Specifically, for almost all vulnerabilities (7/9 for PlanFuzz$^{-\text{guide}}$, and 8/9 for PlanFuzz$^{-\text{PI}}$), the μTTE performance drops are *statistically significant* (bold $\hat{A}_{12}$ values in Table III). From the μTTE values, PlanFuzz$^{-\text{guide}}$ and PlanFuzz$^{-\text{PI}}$ are on average *>4.5*$\times$ and *>3.5*$\times$ slower respectively; for complicated cases like V1, such degradation can be even *over 7.7*$\times$ for PlanFuzz$^{-\text{guide}}$. Among the 9 vulnerabilities, V4 is the only one without significant μTTE differences for both PlanFuzz$^{-\text{guide}}$ and PlanFuzz$^{-\text{PI}}$, likely because it is relatively easier to trigger by nature due to a likely range-checking bug, which can be seen by its much lower μTTE values (1 sec). However, even so, without *both* of these problem-specific designs (BP vulnerability distance and PI-aware physical-object generation), they still *cannot* be discovered by traditional fuzzers like PB-M even given 24h (Table III).

VI. Exploitation Case Studies

In this section, we provide three case studies on the BP DoS vulnerabilities discovered by our testing framework and demonstrate how an attacker can exploit the vulnerabilities to disrupt the normal driving behavior of the AD vehicle without raising suspicion. Specifically, we select one vulnerability from each of the attack scenarios categorized in §V-B. The case studies are conducted in an end-to-end way, where we create the concrete driving environments with the attack obstacles in an AD simulator, LGSVL [96], and simulate with

Table III: Results of baseline comparison. PlanFuzz$^{-\text{guide}}$: PlanFuzz without BP vulnerability distance as guidance. PlanFuzz$^{-\text{PI}}$: PlanFuzz without PI-aware physical-object generation. PB-M: Protobuf-mutator (a directly-compatible traditional fuzzer). Each setup is run 10 times, 24h each time. μTTE is average Time-To-Exposure. NF: Vulnerability not found in 24h. **Bold** $\hat{A}_{12}$ values denote statistically significant μTTE performance drops.

Seed	Uniq. vuln	PlanFuzz μTTE	PlanFuzz$^{-\text{guide}}$ μTTE	PlanFuzz$^{-\text{guide}}$ $\hat{A}_{12}$	PlanFuzz$^{-\text{PI}}$ μTTE	PlanFuzz$^{-\text{PI}}$ $\hat{A}_{12}$	PB-M μTTE
1	V1	165s	1278s (7.74×)	**0.97**	276s (1.67×)	**0.88**	NF
2	V2	19s	21s (1.11×)	0.55	117s (6.15×)	**0.98**	NF
3	V3	16s	34s (2.12×)	**0.88**	53s (3.31×)	**0.88**	NF
	V4	1s	1s (1.00×)	0.57	2s (2.00×)	0.58	NF
4	V5	47s	92s (1.95×)	**0.89**	167s (3.55×)	**0.98**	NF
	V6	35s	78s (2.22×)	**0.83**	148s (4.22×)	**0.93**	NF
5	V7	45s	119s (2.64×)	**0.97**	208s (4.62×)	**0.96**	NF
6	V8	53s	193s (3.64×)	**0.96**	327s (6.16×)	**0.90**	NF
7	V9	37s	57s (1.54×)	**0.93**	188s (5.08×)	**0.96**	NF
Average		46s	208s (4.52×)	**0.83**	165s (3.58×)	**0.89**	NF

the complete AD stack (Apollo or Autoware) in the loop more than 10 times, which also include other AD system components such as localization, perception, and control. We create attack demos for all the case studies listed in this section. Demo videos are available at our project website **https://sites.google.com/view/cav-sec/planfuzz** [33].

A. Lane Following DoS Attack on Autoware

Vulnerable decision logic. The lane following DoS attack on Autoware (V8) is able to change the AD vehicle's lane following decision into an overly-conservative decision to permanently stop on a clear road, by exploiting the vulnerable decision logic in `trajectory_evaluator` in Autoware. This evaluator is designed to decide whether there is a candidate trajectory for AD vehicle to safely pass without crashing into a static obstacle. Similar to Apollo's design illustrated in §III-A, Autoware predefined an overly-conservative lateral safety buffer of 1.2 meters between the AD vehicle and any obstacles. As described in §III-A, since the minimal urban lane width is 2.7m and typical width of AD vehicle (with mirrors) is larger than 2m, two static obstacles out of lane boundaries can block all the candidate trajectories for the AD vehicle.

Exploitation method. To exploit this vulnerability, the attacker can find a single-lane road up to 4.35m wide (applicable to both common local and highway roads [66]), and put two easy-to-carry objects, e.g., cardboard boxes, on each side of the road. There is no strict relative longitudinal position requirement for them, as long as they are in the same planning range (35m for Autoware). Since Autoware uses a more conservative safety buffer size than Apollo, for a narrow road width such as 2.7m [66], each of such object can be >80cm to the road boundary to make them look more stealthy. An example setup in the simulator is shown in Fig. 4 (C). This can cause an emergency stop and/or permanent stop of the victim AD vehicle and thus damage the AD service, block traffic, and also potentially damage road safety (from emergency stop).

End-to-end attack results. We set up the above exploitation scenario in the simulator. From the simulation, after detecting the cardboard boxes, the AD vehicle immediately starts to decelerate and finally comes to a complete stop at ∼10m in front of the boxes. After the full stop, we keep the simulator and AD system running to observe if the AD vehicle will move forward. After waiting for ∼30min, the vehicle still stops at the original position. We manually examined the code and confirmed that this will be a permanent stop. A demo video is at our website [33] and the snapshot when the AD vehicle stops in front of the boxes is in Fig. 4 (C). As shown, the cardboard boxes are located very far from the lane boundaries and the lane is completely clear to drive from the driver's view.

Such a vulnerability can lead to severe congestion and even rear-end collisions if the following vehicle is not able to react in time; video demos are at our website [33]. The attack consequence can be especially severe if launched at critical road segments such as highway exit ramps, or in front of police or fire stations (e.g., to block emergency responder actions).

Physical-world experiment. We further collect attack traces in real world to justify the attack realism. We conduct the experiment with a Lincoln MKZ [108] equipped with Velodyne VLP-32C LiDAR [109] and NovAtel Positioning Kits [110]. We mark a traffic lane with 3.5m width inside the parking lot and use a cardboard box and a trash can to construct the attack scenario. Due to the safety concern, we manually drive the car following the traffic lane to collect the attack trace. We run the Autoware's LiDAR clustering and tracking nodes to get the object detection results and launch the op_planner nodes to get the planning decisions. For all the frames in our collected traces, the two static obstacles can be detected correctly, and the stop decision is made for every single frame in the traces. Thus, we deemed the Autoware's lane following vulnerability reconstructable in real world. Fig. 7 shows our experiment setup and result.

B. Intersection Passing DoS Attack on Apollo

Vulnerable decision logic. This DoS vulnerability (V7) appears in Apollo, where the attacker can force an AD vehicle to stop permanently in front of an intersection with a 4-way stop sign. Apollo BP follows the "first come, first serve" traffic principle when the AD vehicle arrives at a 4-way stop sign. The vehicle maintains a watch list containing all vehicles and bicycles which reaches the intersection earlier than itself and waits until all vehicles and bicycles on that list have left the intersection. However, due to an overly-conservative distance threshold (5m), which is much larger than even the typical *highway* lane width (3.6m [66]), when judging if a vehicle or bicycle is on a lane and waiting for a stop sign, a parked bicycle that is not on the road will be mistakenly added to the watch list, which causes the AD vehicle to unnecessarily wait for off-road objects that are irrelevant to the stop sign-based intersection passing norms.

Exploitation method. To exploit this, the attacker can find any stop sign-based intersections, and place road-side parked bikes as long as they are within 5m from the lane center of any lanes in the intersection. Here, 2 parked bicycles are enough

to bypass all timeout mechanisms in Apollo BP. This can then force the AD vehicles to stop in front of the stop line forever.

End-to-end attack result. We set up the exploitation scenario above in the simulator. Fig. 8 shows the snapshots of the benign and attack demos with and without the 2 parked bicycles. In the benign scenario, the AD vehicle can smoothly proceed and pass the intersection with stop signs. However, in the attack scenario, after the AD vehicle arrives at the intersection, it became stuck in front of the stop sign due to the two roadside parked bicycles despite the intersection being completely empty without any other vehicles.

C. Lane Changing DoS Attack on Apollo

Vulnerable decision logic. The lane-changing DoS attack on Apollo (V2) is able to force the AD vehicle to give up a lane-changing decision by exploiting decision logic in `lane_change_decider` of Apollo. As shown by the pseudo code in Fig. 10, the decision logic determines whether the target lane is clear for performing lane changing by checking if any vehicle occupies the target lane and is close to the AD vehicle. In the code, all the position variables (e.g., `start_l`, `start_s`) are in the Frenet coordinate relative to the target lane. Due to an overly-conservative lateral distance threshold (2.5m in line 5), a nearby vehicle following the AD vehicle or driving on the other adjacent lane will be considered as occupying the target lane and force the AD vehicle to give up the lane-changing decision.

Exploitation method. To exploit this, for lanes with $\leq$3.55m width (applicable to almost all common local and highway lanes (up to 3.6m wide) [66]), the attacker just needs to drive a normal-size car (e.g., 2.11m as in §III-A) to follow a victim AD vehicle with close following distance (up to 8m). This can then prevent the AD vehicle from making lane changes forever, which can make it fail to arrive at the destination (especially critical for AD services such as robo-taxi/delivery). For lanes wider than 3.55m, the attacker just needs to drive with a slight deviation to the lane center (e.g., 5cm for a 3.6m-wide lane, which is far from touching the lane line ($>$70cm)) towards the victim's lane changing direction.

End-to-end attack results. We set up the exploitation scenario above in the simulator. Fig. 9 shows the snapshots of the benign and attack demo videos. In the benign scenario, the AD vehicle can successfully change lanes since the following vehicle's lateral position does not satisfy the vulnerability condition. However, in the attack scenario, although the changing lane is completely empty without any vehicles in the front or back, the AD vehicle still gives up the lane-changing decision to stay on the current lane, which causes it to miss the optimal route to the destination. For AD vehicles, such a BP decision often entails a re-routing step to recalculate a new route to reach the destination. However, since the attacker can simply keep following the AD vehicle and perform such attacks on every new route, it is possible for the AD vehicle to never reach the destination in the worst case.

VII. Discussion and Future works

A. Root Cause and Solution Discussions

Among the vulnerabilities discovered, only 1 (V4) is likely an implementation bug, while the remaining 8 are due to the overly-conservative planning parameters/logic in judging safety. Specifically, V1, V8 are due to overly-conservative safety buffer configuration to road-side static objects; V9 is due to overly-conservative safe buffer configuration to moving vehicle trajectories in other lanes; V2, V3, V5, V6, and V7 are due to the overly-conservative logic in judging the intention of surrounding vehicles (V2, V3), pedestrians (V5, V6), and parked bikes (V7). More details are in extended version [89].

Solution discussions. Based on the causes, V4 can be potentially fixed by a bug patch; the other 8 are harder to fundamentally fix as it is non-trivial to effectively and practically balance the trade-off between safety and availability in an AD context. For example, considering the vulnerability causes are overly-conservative parameters/logic, a direct idea is to just make the design/implementation more aggressive, e.g., reducing the safety buffer configuration to road-side static objects. However, since such existing configurations may already be sufficiently tuned to ensure safety, changing them may compromise safety. One potential design direction for better addressing this trade-off is to consider dynamic configurations instead of fixed ones, e.g., dynamically adjusting the safety margin based on the velocity, since the required safety distance will decrease with a smaller velocity [111] (which is one reason why highway lanes are wider than local ones [112]). However, how to design such dynamic adjustment is non-trivial since various internal and external driving factors need to be systematically considered (e.g., internal ones such as vehicle size/speed, external ones such as the static/dynamic road conditions), which we thus leave as future work.

B. Limitations and Future Work

Tool effectiveness. PlanFuzz's results do not have false positives since all the discovered vulnerabilities have been confirmed by the vulnerability checker. However, similar to all dynamic testing approaches, PlanFuzz cannot give any guarantee on the non-existence of the vulnerability and thus can have false negatives (FNs). Specifically, FNs can come from: (1) the evolutionary algorithm gets stuck at a local minimum or terminate too early. We plan to try other generic optimization algorithms in the future; and (2) the vulnerability only exists in a specific road condition (e.g., a specific road layout and/or surrounding traffic pattern) that is not included in our BP input traces. These vulnerabilities may be arguably less important though as their triggering conditions are narrower. To also capture these, one potential future direction is to also mutate the road conditions. However, how to ensure that the PI still holds after such mutations is a challenge.

Applicability and generality. Due to the limitation of available code bases, we only evaluate the applicability and generality of PlanFuzz on open-source AD systems. Nevertheless, the design of PlanFuzz is general at both design and

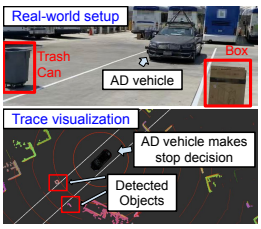

Figure 7: Real-world experiment setup (top) and sensor trace visualization (bottom).

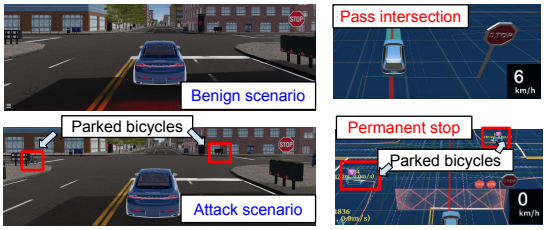

Figure 8: Benign (top): AD vehicle passes the intersection. Attack (bottom): AD vehicle permanently stops because of the parked bicycles placed by the attacker.

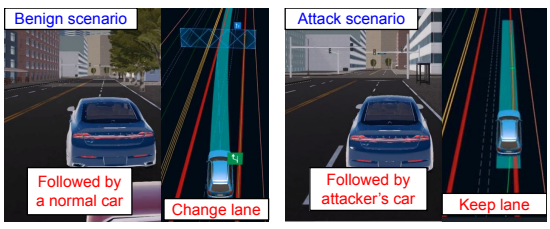

Figure 9: Benign (left): Successfully changes lanes even if it is followed by another vehicle. Attack (right): Fails to change lanes due to the attacker's vehicle.

```
# Iterate over the obstacle list
for (each obs : obstacle_list):
  # Judge based on the lateral position of a veh.
  # start_l, end_l are veh's left/right boundaries
  if (obs.end_l < -2.5 or obs.start_l > 2.5):
    continue
  # The backward safe buffer
  BackwardSafeBuffer ← 4.0f
  # Check whether the veh is close
  if (ego_start_s-obs.end_s<BackwardSafeBuffer):
    IsClearChangeLane ← false
```

Figure 10: Simplified vulnerable pseudo code of V2 (lane changing).

implementation levels. The design of PI and PI-aware physical object mutation does not make any assumption about the AD system designs and implementations under test as long as they are developed for driving on public roads. For the code instrumentation part, we use LLVM [113], which can support a variety of programming languages. Besides, our system should be able to use the gradient to replace BP vulnerability distance if learning-based planners becomes mainstream and easier to interpret, debug, and enforce safety measures in the future.

Stronger threat models. To trigger the semantic DoS vulnerabilities, adding road objects is not the only possible threat model. For example, attackers may also attack the perceptional sensors, such as by sensor spoofing [7] or compromising internal AD system components [114], to introduce malicious inputs to BP. However, the downside is that such attack vectors may also introduce new attack requirements/costs, e.g., sensor spoofing equipment [7] and access to internals or the supply chain of AD systems [114], making the vulnerability exploitation potentially less realistic/practical. We leave the systematic exploration of such a direction to future work.

VIII. Related Work

Autonomous Driving (AD) systems security. Since AD systems heavily rely on sensors, prior works have studied *sensor attacks* in AD context such as sensor spoofing/jamming [6, 7, 115–118]. Besides sensor-level attacks, prior works also studied attacks and defenses of AD system components related to environmental sensing, such as object detection and tracking, localization, and lane detection [5, 7–9, 119–129]. However, so far none of them considered security problems specific to downstream modules such as BP like in this paper.

Vulnerability discovery and property falsification in AD/RV (Robot Vehicle) software. Recently, increasingly more works consider software vulnerabilities/bugs in AD systems [130, 131]. Some developed methods to discover semantic vulnerabilities in the DNN models in AD [7, 9, 23, 24, 119–122, 125, 126, 132, 133]. These methods assume differentiability of the test subject, which thus cannot be applied to the more industry-representative program-based BP targeted in this paper (§II-A). Previous works also falsify safety properties on AD/RV software [10, 28, 73–77, 134]. They cannot be directly applied since the problem scopes are different and the guidance is only limited to black-box guidance.

Vulnerability discovery in RVs, such as drones or rovers, is a closely-related research domain. Compared to AD, RVs typically follow the control commands sent by a base station without the need to make *planning* decisions by itself. Thus, existing works concentrate on control-specific vulnerabilities [25, 26, 28] or highly rely on control-specific knowledge [27, 129], which are orthogonal to the design challenges we need to address for BP-specific vulnerabilities in AD.

IX. Conclusion

In this paper, we design PlanFuzz, a novel dynamic testing approach to systematically discover BP DoS vulnerabilities under physical-world attacks. We propose and identify PIs as novel testing oracles, and design novel problem-specific fuzzing designs such as PI-aware physical-object generation and BP vulnerability distance. We evaluate PlanFuzz on 3 practical BP implementations, and find that it can effectively discover 9 previously-unknown semantic DoS vulnerabilities without false positives. We further perform exploitation case studies, and discuss root causes and potential vulnerability solution directions. We hope that our findings and insights can inspire effective solution designs in future works.

Acknowledgment

We would like to thank Ningfei Wang, Yunpeng Luo, Takami Sato, Junze Liu, and the anonymous reviewers for valuable feedback on our work. This research was supported in part by the NSF under grants CNS-1850533, CNS-1929771, CNS-2145493, CNS-1823262, and CMMI-2054710.

References

[1] S. O.-R. A. V. S. Committee *et al.*, "Taxonomy and Definitions for Terms Related to Driving Automation Systems for On-Road Motor Vehicles," *SAE International: Warrendale, PA, USA*, 2018.

[2] "Waymo is Opening its Fully Driverless Service to the General Public in Phoenix," https://blog.waymo.com/2020/10/waymo-is-opening-its-fully-driverless.html.

[3] "UPS Joins Race for Future of Delivery Services by Investing in Self-driving Trucks," https://tinyurl.com/2p886dud.

[4] "PonyAI Robotaxi Service," https://www.pony.ai/en/index.html.

[5] J. Shen, J. Y. Won, and Q. A. Chen, "Drift with Devil: Security of Multi-Sensor Fusion based Localization in High-Level Autonomous Driving under GPS Spoofing," in *Usenix Security*, 2020.

[6] C. Yulong, W. Ningfei, X. Chaowei, Y. Dawei, F. Jin, Y. Ruigang, C. Qi Alfred, L. Mingyan, and L. Bo, "Invisible for both Camera and LiDAR: Security of Multi-Sensor Fusion based Perception in Autonomous Driving Under Physical-World Attacks," in *S&P*. IEEE, 2021.

[7] Y. Cao, C. Xiao, B. Cyr, Y. Zhou, W. Park, S. Rampazzi, Q. A. Chen, K. Fu, and Z. M. Mao, "Adversarial Sensor Attack on LiDAR-based Perception in Autonomous Driving," in *ACM CCS*, 2019.

[8] J. Sun, Y. Cao, Q. A. Chen, and Z. M. Mao, "Towards robust lidar-based perception in autonomous driving: General black-box adversarial sensor attack and countermeasures," in *USENIX Security*, 2020.

[9] Y. Zhao, H. Zhu, R. Liang, Q. Shen, S. Zhang, and K. Chen, "Seeing isn't Believing: Practical Adversarial Attack Against Object Detectors," *ACM CCS*, 2019.

[10] D. J. Fremont, E. Kim, Y. V. Pant, S. A. Seshia, A. Acharya, X. Bruso, P. Wells, S. Lemke, Q. Lu, and S. Mehta, "Formal Scenario-based Testing of Autonomous Vehicles: From Simulation to the Real World," in *ITSC*. IEEE, 2020.

[11] "Death of Elaine Herzberg," https : / / en.wikipedia.org / wiki / Death_of_Elaine_Herzberg.

[12] "Tesla In Taiwan Crashes Directly Into Overturned Truck, Ignores Pedestrian, With Autopilot On," https://tinyurl.com/r94yvyas.

[13] "Two People Killed in Fiery Tesla Crash with No One Driving," https: //tinyurl.com/2p9a3dat.

[14] "Tesla on Autopilot Crashes into Michigan Cop's Patrol Car," https: //tinyurl.com/2p994vc5.

[15] "Waymo Vehicle Gets Stuck, Then Abandons Me (Also I found a UI bug!) | JJRicks Rides with Waymo 27," https://youtu.be/SH7cQojJlT8.

[16] "Waymo Self Driving: TWO Roadside Assistance Takeovers and MUCH More! | JJRicks Rides With Waymo 21," https://youtu.be/Uy3DuUOLhUE.

[17] "Waymo Self Driving Taxi Fumbles In Construction Zone, Blocks Traffic | JJRicks Rides with Waymo 54," https://youtu.be/zdKCQKBvH-A?t=1036.

[18] "Humans Will Bully Mild-Mannered Autonomous Cars," https : // tinyurl.com/5n8x4whu.

[19] "Uber Says People are Bullying its Self-driving Cars with Rude Gestures and Road Rage," https://www.businessinsider.com/uber-people-bullying-self-driving-cars-2019-6.

[20] "First self-driving cars will be unmarked so that other drivers don't try to bully them," https://www.theguardian.com/technology/2016/oct/30/volvo-self-driving-car-autonomous.

[21] T. Petsios, A. Tang, S. Stolfo, A. D. Keromytis, and S. Jana, "Nezha: Efficient Domain-independent Differential Testing," in *S&P*. IEEE, 2017.

[22] C. Brubaker, S. Jana, B. Ray, S. Khurshid, and V. Shmatikov, "Using Frankencerts for Automated Adversarial Testing of Certificate Validation in SSL/TLS Implementations," in *S&P*. IEEE, 2014.

[23] K. Pei, Y. Cao, J. Yang, and S. Jana, "Deepxplore: Automated Whitebox Testing of Deep Learning Systems," in *SOSP*, 2017.

[24] Y. Tian, K. Pei, S. Jana, and B. Ray, "Deeptest: Automated Testing of Deep-neural-network-driven Autonomous Cars," in *ICSE*, 2018.

[25] T. Kim, C. H. Kim, J. Rhee, F. Fei, Z. Tu, G. Walkup, X. Zhang, X. Deng, and D. Xu, "RVFUZZER: Finding Input Validation Bugs in Robotic Vehicles through Control-guided Testing," in *USENIX Security*, 2019.

[26] H. Choi, S. Kate, Y. Aafer, X. Zhang, and D. Xu, "Cyber-Physical Inconsistency Vulnerability Identification for Safety Checks in Robotic Vehicles," in *ACM CCS*, 2020.

[27] T. Kim, C. H. Kim, A. Ozen, F. Fei, Z. Tu, X. Zhang, X. Deng, D. J. Tian, and D. Xu, "From Control Model to Program: Investigating Robotic Aerial Vehicle Accidents with MAYDAY," in *USENIX Security*, 2020.

[28] H. Kim, M. O. Ozmen, A. Bianchi, Z. B. Celik, and D. Xu, "PGFUZZ: Policy-Guided Fuzzing for Robotic Vehicles," in *NDSS*, 2021.

[29] "Apollo: An Open Autonomous Driving Platform," https://github.com/ApolloAuto/apollo.

[30] S. Kato, S. Tokunaga, Y. Maruyama, S. Maeda, M. Hirabayashi, Y. Kitsukawa, A. Monrroy, T. Ando, Y. Fujii, and T. Azumi, "Autoware On Board: Enabling Autonomous Vehicles with Embedded Systems," in *ICCPS'18*. IEEE Press, 2018, pp. 287–296.

[31] "Navigant Research Names Waymo, Ford Autonomous Vehicles, Cruise, and Baidu the Leading Developers of Automated Driving Systems," https://tinyurl.com/ypt2m6jf.

[32] "Carma Platform," https://github.com/usdot-fhwa-stol/carma-platform.

[33] "PlanFuzz Website," https://sites.google.com/view/cav-sec/planfuzz.

[34] B. Paden, M. Čáp, S. Z. Yong, D. Yershov, and E. Frazzoli, "A Survey of Motion Planning and Control Techniques for Self-driving Urban Vehicles," *IEEE Transactions on intelligent vehicles*, 2016.

[35] M. Ilievski, S. Sedwards, A. Gaurav, A. Balakrishnan, A. Sarkar, J. Lee, F. Bouchard, R. De Iaco, and K. Czarnecki, "Design Space of Behaviour Planning for Autonomous Driving," *arXiv preprint arXiv:1908.07931*, 2019.

[36] C. Urmson, J. Anhalt, D. Bagnell, C. Baker, R. Bittner, M. Clark, J. Dolan, D. Duggins, T. Galatali, C. Geyer *et al.*, "Autonomous Driving in Urban Environments: Boss and the Urban Challenge," *Journal of Field Robotics*, 2008.

[37] M. Buehler, K. Iagnemma, and S. Singh, *The DARPA Urban Challenge: Autonomous Vehicles in City Traffic*. springer, 2009.

[38] D. González, J. Pérez, V. Milanés, and F. Nashashibi, "A Review of Motion Planning Techniques for Automated Vehicles," *IEEE Transactions on Intelligent Transportation Systems*, 2015.

[39] S. D. Pendleton, H. Andersen, X. Du, X. Shen, M. Meghjani, Y. H. Eng, D. Rus, and M. H. Ang, "Perception, Planning, Control, and Coordination for Autonomous Vehicles," *Machines*, 2017.

[40] W. Schwarting, J. Alonso-Mora, and D. Rus, "Planning and Decision-making for Autonomous Vehicles," *Annual Review of Control, Robotics, and Autonomous Systems*, 2018.

[41] L. Sun, C. Peng, W. Zhan, and M. Tomizuka, "A Fast Integrated Planning and Control Framework for Autonomous Driving via Imitation Learning," in *Dynamic Systems and Control Conference*, vol. 51913. American Society of Mechanical Engineers, 2018, p. V003T37A012.

[42] Y. Chen, P. Praveen, M. Priyantha, K. Muelling, and J. Dolan, "Learning on-road Visual Control for Self-driving Vehicles with Auxiliary Tasks," in *WACV*. IEEE, 2019.

[43] P. Abbeel, D. Dolgov, A. Y. Ng, and S. Thrun, "Apprenticeship Learning for Motion Planning with Application to Parking Lot Navigation," in *2008 IEEE/RSJ International Conference on Intelligent Robots and Systems*. IEEE, 2008.

[44] J. Koutník, G. Cuccu, J. Schmidhuber, and F. Gomez, "Evolving Large-Scale Neural Networks for Vision-Based Reinforcement Learning," in *Proceedings of the 15th Annual Conference on Genetic and Evolutionary Computation*, ser. GECCO '13. New York, NY, USA: Association for Computing Machinery, 2013, p. 1061–1068. [Online]. Available: https://doi.org/10.1145/2463372.2463509

[45] S. Wang, D. Jia, and X. Weng, "Deep Reinforcement Learning for Autonomous Driving," *arXiv preprint arXiv:1811.11329*, 2018.

[46] D. Loiacono, A. Prete, P. L. Lanzi, and L. Cardamone, "Learning to Overtake in TORCS using Simple Reinforcement Learning," in *IEEE Congress on Evolutionary Computation*. IEEE, 2010.

[47] E. Capo and D. Loiacono, "Short-Term Trajectory Planning in TORCS using Deep Reinforcement Learning," in *2020 IEEE Symposium Series on Computational Intelligence (SSCI)*. IEEE, 2020.

[48] A. E. Sallab, M. Abdou, E. Perot, and S. Yogamani, "Deep Reinforcement Learning Framework for Autonomous Driving," *Electronic Imaging*, 2017.

[49] B. Osiński, A. Jakubowski, P. Zięcina, P. Miłoś, C. Galias, S. Homoceanu, and H. Michalewski, "Simulation-based reinforcement learning for real-world autonomous driving," in *2020 IEEE International Conference on Robotics and Automation (ICRA)*, 2020, pp. 6411–6418.

[50] A. Kendall, J. Hawke, D. Janz, P. Mazur, D. Reda, J.-M. Allen, V.-D. Lam, A. Bewley, and A. Shah, "Learning to Drive in a Day," in *ICRA*. IEEE, 2019.

[51] A. Kuefler, J. Morton, T. Wheeler, and M. Kochenderfer, "Imitating Driver Behavior with Generative Adversarial Networks," in *IV*. IEEE, 2017.

[52] J. S. H. S. T. Han and B. Zhou, "Neuro-Symbolic Program Search for Autonomous Driving Decision Module Design," in *CoRL*, 2020.

[53] H. Bai, D. Hsu, and W. S. Lee, "Integrated Perception and Planning in the Continuous Space: A POMDP Approach," *The International Journal of Robotics Research*, 2014.

[54] S. Brechtel, T. Gindele, and R. Dillmann, "Solving Continuous POMDPs: Value Iteration with Incremental Learning of an Efficient Space Representation," in *International Conference on Machine Learning*. PMLR, 2013.

[55] K. H. Wray, S. J. Witwicki, and S. Zilberstein, "Online Decision-making for Scalable Autonomous Systems," in *IJCAI*, 2017.

[56] F. Behbahani, K. Shiarlis, X. Chen, V. Kurin, S. Kasewa, C. Stirbu, J. Gomes, S. Paul, F. A. Oliehoek, J. Messias *et al.*, "Learning from Demonstration in the Wild," in *ICRA*. IEEE, 2019.

[57] L. Chi and Y. Mu, "Deep Steering: Learning end-to-end Driving Model from Spatial and Temporal Visual Cues," *arXiv preprint arXiv:1708.03798*, 2017.

[58] E. Yurtsever, J. Lambert, A. Carballo, and K. Takeda, "A Survey of Autonomous Driving: Common Practices and Emerging Technologies," *IEEE Access*, vol. 8, pp. 58 443–58 469, 2020.

[59] "Path Planning Project Udacity Self-driving Car Nanodegree," https://medium.com/intro-to-artificial-intelligence/path-planning-project-udacitys-self-driving-car-nanodegree-be1f531cc4f7.

[60] "Argo Developing a Self-Driving System You Can Trust," https://www.argo.ai/wp-content/uploads/2021/04/ArgoSafetyReport.pdf.

[61] "Tesla under Investigation by SEC after Fatal Crash Involving Autopilot Report," https://www.theguardian.com/technology/2016/jul/11/sec-tesla-self-driving-car-crash-death-investigation.

[62] "Aurora Acquires Uber's Automated Driving Unit–And Uber's Cash," https://tinyurl.com/2aduvnwa.

[63] "Baidu Will Launch Driverless Robotaxis In Beijing This Week," https://tinyurl.com/twd5zbn6.

[64] "Waymo is opening its fully driverless service to the general public in Phoenix," https://blog.waymo.com/2020/10/waymo-is-opening-its-fully-driverless.html.

[65] "Nuro can now operate and charge for autonomous delivery services in California," https://tinyurl.com/2trxzjre.

[66] "USDoT Lane Width," https://safety.fhwa.dot.gov/geometric/pubs/mitigationstrategies/chapter3/3_lanewidth.cfm.

[67] "Automotive Platforms," https://autonomoustuff.com/products/astuff-automotive.

[68] "Ford Fusion/Fusion Hybrid Features And Specs," https://www.caranddriver.com/ford/fusion/specs.

[69] "Lincoln MKZ Features And Specs," https://www.caranddriver.com/lincoln/mkz/specs.

[70] "Jaguar I-Pace Wiki," https://en.wikipedia.org/wiki/Jaguar_I-Pace.

[71] "California Driver Handbook," https://www.dmv.ca.gov/portal/handbook/california-driver-handbook/laws-and-rules-of-the-road/.

[72] "Vehicle Code 22500 CVC – Improper Parking, Stopping or Standing," https://www.shouselaw.com/ca/defense/vehicle-code/22500.

[73] D. J. Fremont, J. Chiu, D. D. Margineantu, D. Osipychev, and S. A. Seshia, "Formal Analysis and Redesign of a Neural Network-based Aircraft Taxiing System with VerifAI," in *CAV*, 2020.

[74] T. Dreossi, D. J. Fremont, S. Ghosh, E. Kim, H. Ravanbakhsh, M. Vazquez-Chanlatte, and S. A. Seshia, "Verifai: A Toolkit for the Formal Design and Analysis of Artificial Intelligence-based Systems," in *CAV*, 2019.

[75] T. Dreossi, A. Donzé, and S. A. Seshia, "Compositional Falsification of Cyber-physical Systems with Machine Learning Components," *Journal of Automated Reasoning*, 2019.

[76] M. Hekmatnejad, B. Hoxha, and G. Fainekos, "Search-based Test-case Generation by Monitoring Responsibility Safety Rules," in *ITSC*. IEEE, 2020.

[77] C. E. Tuncali, G. Fainekos, H. Ito, and J. Kapinski, "Simulation-based Adversarial Test Generation for Autonomous Vehicles with Machine Learning Components," in *IV*. IEEE, 2018.

[78] D. J. Fremont, T. Dreossi, S. Ghosh, X. Yue, A. L. Sangiovanni-Vincentelli, and S. A. Seshia, "Scenic: A Language for Scenario Specification and Scene Generation," in *PLDI*, 2019.

[79] G. Klees, A. Ruef, B. Cooper, S. Wei, and M. Hicks, "Evaluating Fuzz Testing," in *CCS*. ACM, 2018.

[80] H. Chen, Y. Xue, Y. Li, B. Chen, X. Xie, X. Wu, and Y. Liu, "Hawkeye: Towards a Desired Directed Grey-box Fuzzer," in *ACM CCS*, 2018.

[81] V.-T. Pham, M. Böhme, A. E. Santosa, A. R. Caciulescu, and A. Roychoudhury, "Smart Greybox Fuzzing," *TSE*, 2019.

[82] M. Böhme, V.-T. Pham, and A. Roychoudhury, "Coverage-based Greybox Fuzzing as Markov Chain," *TSE*, 2017.

[83] A. Fioraldi, D. C. D'Elia, and E. Coppa, "WEIZZ: Automatic Grey-box Fuzzing for Structured Binary Formats," in *ISSTA*, 2020.

[84] S. Rawat, V. Jain, A. Kumar, L. Cojocar, C. Giuffrida, and H. Bos, "VUzzer: Application-aware Evolutionary Fuzzing," in *NDSS*, 2017.

[85] S. Sparks, S. Embleton, R. Cunningham, and C. Zou, "Automated Vulnerability Analysis: Leveraging Control Flow for Evolutionary Input Crafting," in *ACSAC*. IEEE, 2007.

[86] S. Rawat and L. Mounier, "An Evolutionary Computing Approach for Hunting Buffer Overflow Vulnerabilities: A Case of Aiming in Dim Light," in *2010 European Conference on Computer Network Defense*. IEEE, 2010.

[87] D. Whitley, "A Genetic Algorithm Tutorial," *Statistics and Computing*, vol. 4, no. 2, pp. 65–85, 1994.

[88] "General Motors 2018 Self-Driving Safety Report," https://tinyurl.com/43kjm6dc.

[89] "Extended Version of this Paper," https://arxiv.org/abs/2201.04610.

[90] M. Böhme, V.-T. Pham, M.-D. Nguyen, and A. Roychoudhury, "Directed Greybox Fuzzing," in *ACM CCS*, 2017.

[91] "Autoware Self-driving Vehicle on a Highway," https://www.youtube.com/watch?v=npQMzH3j_d8.

[92] "Baidu Launches Their Open Platform for Autonomous Cars and We Got to Test it," https://technode.com/2017/07/05/baidu-apollo-1-0-autonomous-cars-we-test-it/.

[93] "Baidu Apollo Release," https://github.com/ApolloAuto/apollo/releases.

[94] "Autoware.AI," https://www.autoware.ai/.

[95] H. Darweesh, E. Takeuchi, K. Takeda, Y. Ninomiya, A. Sujiwo, L. Y. Morales, N. Akai, T. Tomizawa, and S. Kato, "Open-source Integrated Planner for Autonomous Navigation in Highly Dynamic Environments," *Journal of Robotics and Mechatronics*, 2017.

[96] LG, "LGSVL Simulator: An Autonomous Vehicle Simulator," https://github.com/lgsvl/simulator.

[97] "Simulation Becomes Increasingly Important For Self-Driving Cars," https://www.forbes.com/sites/davidsilver/2018/11/01/simulation-becomes-increasingly-important-for-self-driving-cars/.

[98] "Inside Waymo's Secret World for Training Self-Driving Cars," https://www.theatlantic.com/technology/archive/2017/08/inside-waymos-secret-testing-and-simulation-facilities/537648/.

[99] "Simulation Engine from MIT Trains Self-Driving Cars Before They Hit Real Roads," https://www.therobotreport.com/simulation-engine-mit-trains-self-driving-cars-before-hit-real-streets/.

[100] "Tesla's Sensor Coverage (Almost 306 Degree Coverage at 80m)," https://www.tesla.com/autopilot.

[101] "AFL," http://lcamtuf.coredump.cx/afl.

[102] I. Yun, S. Lee, M. Xu, Y. Jang, and T. Kim, "QSYM: A Practical Concolic Execution Engine Tailored for Hybrid Fuzzing," in *USENIX Security*, 2018.

[103] P. Chen and H. Chen, "Angora: Efficient Fuzzing by Principled Search," in *S&P*. IEEE, 2018.

[104] N. Stephens, J. Grosen, C. Salls, A. Dutcher, R. Wang, J. Corbetta, Y. Shoshitaishvili, C. Kruegel, and G. Vigna, "Driller: Augmenting Fuzzing Through Selective Symbolic Execution," in *NDSS*, 2016.

[105] "Protobuf-Mutator," https://github.com/google/libprotobuf-mutator.

[106] G. Klees, A. Ruef, B. Cooper, S. Wei, and M. Hicks, "Evaluating Fuzz Testing," in *ACM CCS*, 2018.

[107] A. Arcuri and L. Briand, "A Practical Guide for Using Statistical Tests to Assess Randomized Algorithms in Software engineering," in *ICSE*. IEEE, 2011.

[108] "Lincoln MKZ Datasheet," https://autonomoustuff.com/-/media/Images/Hexagon/Hexagon%20Core/autonomousstuff/pdf/as-lincoln-mkz-datasheet.ashx.

[109] "Velodyne LiDAR's ULTRA Puck VLP-32C," https://tinyurl.com/5b2sdj8c.

[110] "NovAtel Positioning Kits," https://tinyurl.com/7acmrjdc.

[111] S. Shalev-Shwartz, S. Shammah, and A. Shashua, "On a Formal Model of Safe and Scalable Self-Driving Cars," *arXiv preprint arXiv:1708.06374*, 2017.

[112] "Urban Street Design Guide," https://tinyurl.com/2p96dnur.

[113] "LLVM Project," https://llvm.org/.

[114] S. Jha, S. Cui, S. Banerjee, J. Cyriac, T. Tsai, Z. Kalbarczyk, and R. K. Iyer, "Ml-Driven Malware that Targets AV Safety," in *DSN*. IEEE, 2020.

[115] C. Yan, W. Xu, and J. Liu, "Can You Trust Autonomous Vehicles: Contactless Attacks against Sensors of Self-driving Vehicle," *DEF CON*, 2016.

[116] B. Nassi, D. Nassi, R. Ben-Netanel, Y. Mirsky, O. Drokin, and Y. Elovici, "Phantom of the ADAS: Phantom Attacks on Driver-Assistance Systems," in *IACR*, 2020.

[117] H. Shin, D. Kim, Y. Kwon, and Y. Kim, "Illusion and Dazzle: Adversarial Optical Channel Exploits Against LiDARs for Automotive Applications," in *International Conference on Cryptographic Hardware and Embedded Systems*. Springer, 2017, pp. 445–467.
[118] Y. Tu, Z. Lin, I. Lee, and X. Hei, "Injected and Delivered: Fabricating Implicit Control over Actuation Systems by Spoofing Inertial Sensors," in *USENIX Security*, 2018, pp. 1545–1562.
[119] T. Sato, J. Shen, N. Wang, Y. Jia, X. Lin, and Q. A. Chen, "Dirty Road Can Attack: Security of Deep Learning based Automated Lane Centering under Physical-World Attack," in *USENIX Security*, 2021.
[120] T. Sato, J. Shen, N. Wang, Y. J. Jia, X. Lin, and Q. A. Chen, "Deployability Improvement, Stealthiness User Study, and Safety Impact Assessment on Real Vehicle for Dirty Road Patch Attack," in *AutoSec Workshop at NDSS*, 2021.
[121] Y. Cao, N. Wang, C. Xiao, D. Yang, J. Fang, R. Yang, Q. A. Chen, M. Liu, and B. Li, "Invisible for both Camera and LiDAR: Security of Multi-Sensor Fusion based Perception in Autonomous Driving Under Physical World Attacks," in *IEEE S&P*, 2021.
[122] H. Liang, R. Jiao, T. Sato, J. Shen, Q. A. Chen, and Q. Zhu, "End-to-End Analysis of Adversarial Attacks to Automated Lane Centering Systems," in *AutoSec Workshop at NDSS*, 2021.
[123] K. Tang, J. Shen, and Q. A. Chen, "Fooling Perception via Location: A Case of Region-of-Interest Attacks on Traffic Light Detection in Autonomous Driving," in *AutoSec Workshop at NDSS*, 2021.
[124] Y. Jia, Y. Lu, J. Shen, Q. A. Chen, H. Chen, Z. Zhong, and T. Wei, "Fooling Detection Alone is Not Enough: Adversarial Attack Against Multiple Object Tracking," in *ICLR*, 2019.
[125] K. Eykholt, I. Evtimov, E. Fernandes, B. Li, A. Rahmati, F. Tramer, A. Prakash, T. Kohno, and D. Song, "Physical Adversarial Examples for Object Detectors," in *WOOT*, 2018.
[126] S.-T. Chen, C. Cornelius, J. Martin, and D. H. P. Chau, "Shapeshifter: Robust Physical Adversarial Attack on Faster R-CNN Object Detector," in *ECML PKDD*, 2018.
[127] "Model Hacking ADAS to Pave Safer Roads for Autonomous Vehicles," https://tinyurl.com/2r7yfkmu, 2020.
[128] R. Quinonez, J. Giraldo, L. Salazar, E. Bauman, A. Cardenas, and Z. Lin, "Savior: Securing autonomous vehicles with robust physical invariants," in *USENIX Security*, 2020.
[129] H. Choi, W.-C. Lee, Y. Aafer, F. Fei, Z. Tu, X. Zhang, D. Xu, and X. Deng, "Detecting Attacks against Robotic Vehicles: A control Invariant Approach," in *ACM CCS*, 2018.
[130] J. Garcia, Y. Feng, J. Shen, S. Almanee, Y. Xia, and Q. A. Chen, "A Comprehensive Study of Autonomous Vehicle Bugs," in *ICSE*, 2020.
[131] D. K. Hong, J. Kloosterman, Y. Jin, Y. Cao, Q. A. Chen, S. Mahlke, and Z. M. Mao, "AVGuardian: Detecting and Mitigating Publish-Subscribe Overprivilege for Autonomous Vehicle Systems," in *EuroS&P*, 2020.
[132] H. Zhou, W. Li, Z. Kong, J. Guo, Y. Zhang, B. Yu, L. Zhang, and C. Liu, "Deepbillboard: Systematic Physical-world Testing of Autonomous Driving Systems," in *ICSE*. IEEE, 2020.
[133] M. Zhang, Y. Zhang, L. Zhang, C. Liu, and S. Khurshid, "DeepRoad: GAN-based Metamorphic Testing and Input Validation Framework for Autonomous Driving Systems," in *ASE*. IEEE, 2018.
[134] G. Li, Y. Li, S. Jha, T. Tsai, M. Sullivan, S. K. S. Hari, Z. Kalbarczyk, and R. Iyer, "AV-FUZZER: Finding Safety Violations in Autonomous Driving Systems," in *ISSRE*. IEEE, 2020.

APPENDIX A
SUMMARY OF PLANNING INVARIANT

We introduce the formal definition of constraints on physical objects commonly used among different driving scenarios. Note that more customized properties are needed for specific scenarios. When processing the geometry relationship among the objects, AD vehicle, and the road, a necessary step is to transform the position of a physical object from a unified coordinate system (UTM coordinate system in Apollo and Autoware) into a coordinate system relative to a certain lane. We define such functionality as the following function:

$$(s, l, laneID) = transform(pos, m) \tag{3}$$

We define the function with input position pos in UTM coordinate system and the map (m). The outputs of this function are longitudinal position (s) and lateral position (l) relative to the closest lane, and the ID of the closest lane ($laneID$). We do not expand this function in a formal way since this involves more than one thousand lines of source code in Apollo.

We now introduce the constraints of physical objects in detail. For the static objects, the most common constraint is that the static objects should be off the road and should not intersect with any lane boundary. This can be formally defined based on a specific static physical object x and a set of polygon points of its boundary $x.polygon$:

$$\begin{aligned} &StaticOffRoad(x) := \\ &\wedge_{p \in x.polygon} |transform(p, m).l| > halfLaneWidth \end{aligned} \tag{4}$$

This means every polygon point of the object boundary is not within the range of any lane. The ***halfLaneWidth*** also needs to be queried from the map. For simplicity, we just describe it as a constant. For a pedestrian x, we want to make sure that it will not touch any lane in its future moving trajectory and does not show any intention to enter the traffic lane or intersection. In this case, for a pedestrian x, the waypoints set $x.W$ to describe its moving trajectory, $x.polygons(w)$ for the polygon points at waypoint w, the constraints for the pedestrian can be defined as:

$$\begin{aligned} &DynamicOffRoad(x) := \\ &\left(\wedge_{w \in x.W} (\wedge_{p \in x.polygon(w)} |transform(p, m).l| > halfLaneWidth)\right) \\ &\wedge (innerProduct(x.heading, directionTowardsLane) < 0) \end{aligned} \tag{5}$$

The property $DynamicOffRoad$ will check all the waypoints in the future moving trajectory of a physical object x and make sure that any points on the boundary shall not touch the lane boundary. Besides, it also checks the heading of the moving trajectory is not towards to the lane.

There are two possible constraints for a vehicle. First, a vehicle can simply follow the AD vehicle, and it should not affect the planning behavior. For simplicity, we also use a property $driveInLane(x, laneID)$ to describe that the vehicle x keeps driving within the lane denoted by the lane ID ($laneID$). This can be modeled as:

$$\begin{aligned} &FollowVehicle(x) := \\ &(transform(x.pos, m).laneID == ego.laneID) \\ &\wedge (transform(x.pos, m).s + safetyFollowingDistance < ego.s) \\ &\wedge (x.velocity \leq ego.velocity) \\ &\wedge driveInLane(x, transform(x.pos, m).laneID) \end{aligned} \tag{6}$$

Another possibility is that the vehicle is driving normally on another lane. We formally define it as:

$$\begin{aligned} &IrrevalentVehicle(x) := \\ &(transform(x.pos, m).laneID \neq ego.laneID) \\ &\wedge driveInLane(x, transform(x.pos, m).laneID) \end{aligned} \tag{7}$$

Table IV: Summary of Planning Invariants (PI) identified and used in the paper.

PI Index	Planning Scenario	Object Type	Constraints on Physical Objects	Desired Planning Behavior
PI1	Lane following (single-lane road)	Static obstacles Vehicles Pedestrians	**PI-C1.** Off-road and w/o any violation of the boundaries of the lanes the AD vehicle plans to drive on **PI-C2.** Follow the AD vehicle **PI-C3.** Drive on reverse lane **PI-C4+5.** Off-road and w/o any intention to move towards to the AD vehicle or the lanes the AD vehicle plans to drive on	Keep cruising in the current lane
PI2	Lane following (multiple-lane road)	Static obstacles Vehicles Pedestrians	**PI-C1.** Off-road and w/o any violation of the boundaries of the lanes the AD vehicle plans to drive on **PI-C2.** Follow the AD vehicle **PI-C3.** Drive on other lanes **PI-C4+5.** Off-road and w/o any intention to move towards to the AD vehicle or the lanes the AD vehicle plans to drive on	Keep cruising in the current lane
PI3	Lane changing	Static obstacles Vehicles Pedestrians	**PI-C1.** Off-road and w/o any violation of the boundaries of the lanes the AD vehicle plans to drive on **PI-C2.** Follow the AD vehicle **PI-C3.** Drive on other lanes except current and targeted lanes **PI-C4+5.** Off-road and w/o any intention to move towards to the AD vehicle or the lanes the AD vehicle plans to drive on	Finish changing to the targeted lane
PI4	Lane borrow (due to a blocking obstacle)	Static obstacles Vehicles Pedestrians	**PI-C1.** Off-road and w/o any violation of the boundaries of the lanes the AD vehicle plans to drive on **SP-PI-C1.** On-lane and in front of the blocking obstacle **PI-C2.** Follow the AD vehicle **PI-C3.** Drive on other lanes except current and targeted lanes **SP-PI-C2.** On-lane and park in front of the blocking obstacle **PI-C4+5.** Off-road and w/o any intention to move towards to the AD vehicle or the lanes the AD vehicle plans to drive on	Finish borrowing the reverse lane and pass blocking vehicle
PI5	Intersection w/ stop sign	Static obstacles Vehicles Pedestrians	**PI-C1.** Off-road and w/o any violation of the boundaries of the lanes the AD vehicle plans to drive on and the intersection the AD vehicle is going to pass **PI-C2.** Follow the AD vehicle **PI-C3.** Drive on other lanes except current and targeted lanes **PI-C4+5.** Off-road and w/o any intention to move towards to the AD vehicle or the lanes the AD vehicle plans to drive on	Pass intersection w/ stop sign following the traffic rule
PI6	Intersection w/ traffic signal	Static obstacles Vehicles Pedestrians	**PI-C1.** Off-road and w/o any violation of the boundaries of the lanes the AD vehicle plans to drive on and the intersection the AD vehicle is going to pass **PI-C2.** Follow the AD vehicle **PI-C3.** Drive on other lanes except current and targeted lanes **PI-C4+5.** Off-road and w/o any intention to move towards to the AD vehicle or the lanes the AD vehicle plans to drive on	Pass intersection w/ traffic signal following the traffic rule
PI7	Bare intersection	Static obstacles Vehicles Pedestrians	**PI-C1.** Off-road and w/o any violation of the boundaries of the lanes the AD vehicle plans to drive on and the intersection the AD vehicle is going to pass **PI-C2.** Follow the AD vehicle **PI-C3.** Drive on other lanes except current and targeted lanes **PI-C4+5.** Off-road and w/o any intention to move towards to the AD vehicle or the lanes the AD vehicle plans to drive on	Pass the bare intersection
PI8	Parking	Static obstacles Vehicles Pedestrians	**SP-PI-C3.** Placed on other parking spots **SP-PI-C4.** Parked on other parking spots **SP-PI-C5.** Walking pedestrians moving away from AD vehicle	Park into an empty targeted parking spot